Carcinogenesis vol.27 no.9 pp.1812–1827, 2006
doi:10.1093/carcin/bgl009
Advance Access publication March 7, 2006

Dihydroxyphenylethanol induces apoptosis by activating serine/threonine protein phosphatase PP2A and promotes the endoplasmic reticulum stress response in human colon carcinoma cells

Cécile Guichard†, Eric Pedruzzi†, Michèle Fay, Jean-Claude Marie, Françoise Braut-Boucher, Fanny Daniel, Alain Grodet, Marie-Anne Gougerot-Pocidalo, Eric Chastre, Larissa Kotelevets, Gérard Lizard[1], Alain Vandewalle, Fathi Driss[2] and Eric Ogier-Denis*

INSERM, U773, Centre de Recherche Bichat Beaujon CRB3, and Université Paris 7 Denis Diderot, site Bichat, BP 416, F-75018, Paris, France, [1]INSERM U498 CHU du Bocage, Laboratoire de Biochimie Médicale, BP77908, 21019 Dijon Cedex, France and [2]Hôpital X. Bichat, Service de Biochimie Hormonale et Génétique, 46 rue Henri Huchard, 75018 Paris, France

*To whom correspondence should be addressed. Tel. +33 1 4485 6211; Fax: +33 1 4485 6207;
Email: ogier@bichat.inserm.fr

The search for effective chemopreventive compounds is a major challenge facing research into preventing the progression of cancer cells. The naturally occurring polyphenol antioxidants look very promising, but their mechanism of action still remains poorly understood. Here, we show that 2-(3,4-dihydroxyphenyl)ethanol (DPE), a phenol antioxidant derived from olive oil, induces growth arrest and apoptosis in human colon carcinoma HT-29 cells. The mechanisms involve prolonged stress of the endoplasmic reticulum (ER) leading to the activation of the two main branches of the unfolded protein response (UPR), including the Ire1/XBP-1/GRP78/Bip and PERK/eIF2α arms. DPE treatment led to overexpression of the pro-apoptotic factor CHOP/GADD153 and persistent activation of the Jun-NH_2-terminal kinase/activator protein-1 signaling pathway. DPE concomitantly modulated the extracellular signal-regulated kinase 1/2 and Akt/PKB pro-survival factors by altering their phosphorylation status as well as inhibiting tumor necrosis factor-α-induced nuclear factor-κB activation by inactivating the phosphorylation of nuclear factor inhibitor-κB kinase. These findings prompted us to investigate the possible involvement of phosphatases in DPE-mediated action. Using phosphatase inhibitors and RNA interference to silence the Ser/Thr phosphatase 2A (PP2A) prevented DPE-induced cell death. These findings demonstrate that DPE specifically activates PP2A, which plays a key initiating role in various pathways that lead to apoptosis in colon cancer cells.

Abbreviations: Akt/PKB, Akt-dependent activation of protein kinase B; AP-1, activator protein-1; CHOP, C/EBP homologous transcription factor; DPE, 2-(3,4-dihydroxyphenyl)ethanol; eIF2α, subunit of translation initiation factor-2; EOR, ER overload response; ER, endoplasmic reticulum; $Erk_{1/2}$, extracellular sigal-regulated kinase 1/2; GADD153, growth arrest and DNA damage inducible gene 153; JNK, c-Jun NH_2-terminal kinase; PERK, phosphorylation of the ER transducer protein kinase; PP1 and PP2A, Ser/Thr phosphatases 1 and 2A; PP2A-C, recombinant PP2A catalytic subunit; ROS, reactive oxygen species; TNF-α, tumor necrosis factor−α; UPR, unfolded protein response.

†These authors contributed equally to this work.

Introduction

Neoplastic progression of cancer cells is associated with chromosome damage that allows cells to escape from growth and proliferation controls and disables apoptosis. Having accumulated mutations that overcome cell cycle and apoptosis checkpoints, the main obstacle to survival faced by a proliferative cancer cell is the restricted availability of nutrients and oxygen. These conditions encountered by poorly vascularized solid tumors are known to alter the physiological environment of the endoplasmic reticulum (ER), leading to the accumulation of misfolded proteins. This process compromises cell function and activates a range of cellular stress responses, known collectively as ER stress (1). ER stress leads to the activation of complex signaling pathway(s) known as the unfolded protein response (UPR). This response includes the transcriptional activation of genes that encode ER chaperone proteins such as GRP78/Bip, to increase protein-folding capacity within the ER (2), and the upregulation of an ER-associated degradation (ERAD) mechanism, such as the activation of ER degradation-enhanced α-mannosidase-like protein (EDEM), to eliminate misfolded proteins by the ubiquitin–proteasome degradation pathway (3,4). UPR promotes an adaptive response, known as the ER overload response (EOR) (5), which involves activation of the nuclear transcription factor NF-κB, which is known to be a mediator of immune and anti-apoptotic responses, or conversely the activation of apoptotic pathway(s), when the adaptive responses are not sufficient to relieve the ER stress. Several mechanisms appear to contribute to apoptosis in response to ER stress. These include the activation of c-Jun NH_2-terminal kinase (JNK) (6), of the C/EBP homologous transcription factor CHOP/GADD153 (growth arrest and DNA damage inducible gene 153) (7), and/or the activation of the ER-associated caspase 12 (8).

Several studies have suggested that UPR may play a pivotal role in tumor growth (for review see refs 9 and 10). Prolonged activation of the UPR can limit damage and ultimately protect the organism by inducing apoptosis in non-cancerous cells experiencing stress, but how tumor cells can adapt to long-term ER stress still remains largely unknown. The progression of tumor cells results from an imbalance between cell growth and cell death and the chemopreventive drugs that target the apoptotic pathways in premalignant cells have been developed. However, their modes of action, presumably through interactions with ER stress, still remain largely unknown. Since the induction of an ER stress response could potentially produce either protective or destructive effects, it is essential to fully characterize which pathway (i.e. adaptive or apoptosis) and which downstream genes are activated when evaluating the chemopreventive potential of drugs or nutritional and dietary factors.

Dietary polyphenol antioxidant molecules including catechins from green tea, resveratrol from red wine, flavonoids and

quertecin from food products have been shown to diminish the risk of cancer at various anatomical sites and to be potent cancer chemopreventing agents (for review see ref. 11). For example, epigallocatechin induces cell death (12) via the inhibition of mitogen-activated protein kinase (MAPK) signaling (13,14), vascular epithelial growth factor (VEGF)-mediated signaling and subsequent angiogenesis (15), cyclin-dependent kinase activation of activator protein-1 (AP-1) and inhibition of NF-κB activation (16), Akt-dependent activation of Bad (13) and inhibition of cell proliferation by binding to vimentin (17). Resveratrol, another polyphenol found in grape skins, has also been shown to induce upregulation of p21Cip1/WAF1, p53 and Bax and concomitant downregulation of cyclins D1 and E and anti-apoptotic Bcl-2, leading to arrest of the cell cycle in various *in vitro* and *in vivo* models (18). Resveratrol has been shown to suppress the activation of NF-κB, AP-1 and egr-1 transcription factors, and to inhibit protein kinase signaling pathways (for review see ref. 10).

Among the most generally accepted correlations between dietary habits and cancer risk, the 'Mediterranean diet', including olive oil consumption, has been shown to be associated with significant reductions in coronary heart disease as well as in breast, liver and colon cancer and it has been suggested that uncontrolled free radical production may be involved in this effect (19–21). Among the antioxidants in olive oil, hydroxytyrosol or 2-(3,4-dihydroxyphenyl)ethanol (DPE) has a remarkable protective effect against oxidative stress-related damage. It has been shown to prevent low-density lipoprotein oxidation (22), platelet aggregation (23) and to counteract the cytotoxicity caused by reactive oxygen species (ROS) by exerting a scavenging action with respect to ROS generation (24) in various cultured human cell systems (25). In human myeloid leukaemia HL-60 cells, Della Ragione *et al*. (26) have reported that DPE activates apoptosis by causing cytochrome *c* release from mitochondria, by increasing JNK-dependent Bcl-2 phosphorylation and by upregulating several genes, including *c-Jun*, *JNK*, *GADD45*, *TGFβ* and *egr-1* (27). Fabiani *et al*. (28) demonstrated that DPE arrested the cells in the G_0/G_1 phase with a concomitant decrease in the cell percentage in the S-and G_2/M-phases. DPE interferes with the generation of leukotriene from arachidonic acid by inhibiting 5- and 12-lipoxygenases (29). DPE has also been found to exert an inhibitory action on peroxynitrite-dependent DNA base modification and tyrosine nitration (30). Interestingly, at the same concentration DPE did not affect the cell growth of freshly isolated human lymphocytes or polymorphonuclear cells.

The question arises as to whether the anti-proliferative and apoptotic actions of dietary polyphenols are associated with ER stress signaling pathways. In the present study, we investigated the effects of DPE on the proliferative capacities of a range of human colon carcinoma cells in culture and its effects on ER stress. We show that DPE induced both ER stress-dependent adaptative and apoptotic processes in colon adenocarcinoma HT-29 cells. We provide direct evidence that apoptosis induced by DPE is strongly inhibited firstly by okadaic acid and calyculin A, both of which are inhibitors of Ser/Thr phosphatases, and secondly by silencing of Ser/Thr phosphatase 2A (PP2A) expression via an RNA interference strategy. In addition, *in vitro* assays have indicated that DPE specifically activates PP2A. Therefore, PP2A seems to play a pivotal role in regulating the signaling pathways involved in apoptosis induced by DPE. These mechanistic findings strongly suggest that the activation of PP2A by DPE in colon carcinoma cells account for the ability of this polyphenol to trigger apoptosis, and thus extend the link between nutrition and human colon cancer.

Materials and methods

Reagents

Annexin V-FITC, propidium iodide (PI), Z-VAD-fmk, Z-DEVD-fmk, ApoAlert Cell Fractionation Kit, mouse anti-GRP78/Bip, anti-Bcl-2, anti-Bax monoclonal antibodies (Mabs) were from Becton-Dickinson (Le Pont de Claix, France). Nucleospin RNA II kit was from Macherey-Nagel (Hoerdt, France). Superscript II reverse transcriptase was from Invitrogen (Cergy-Pontoise, France). Luciferase Assay System was from Promega (Charbonnières les Bains, France). Mouse anti-CHOP/GADD153 Mab was from Tebu-Bio (Le Perray en Yvelines, France), mouse anti-c-jun/AP-1 (Ab3) and rabbit anti-c-jun phospho-specific (Ser^{73}), anti-SAPK/JNK, anti-SAPK/JNK phospho-specific (Thr^{183} and Tyr^{185}) were from Calbiochem (La Jolla, CA). Mouse anti-β-actin Mab was from Sigma (St Louis, MO). Rabbit anti-$Erk_{1/2}$ was from Santa Cruz Biotechnology (CA). Rabbit polyclonal anti-cleaved caspase 3 (Asp^{175}), anti-Bak, anti-Akt/PKB, anti-Akt/PKB phospho-specific (Ser^{473}), anti-eIF2α, anti-eIF2α phospho-specific (Ser^{51}), anti-$Erk_{1/2}$ phospho-specific (Thr^{202}/Tyr^{204}), anti-IKKβ phospho-specific ($Ser^{176/180}$), anti-PERK phospho-specific (Thr^{980}), anti-GSK3β phospho-specific (Ser^{136}), mouse anti-Bad phospho-specific (Ser^{9}), anti-PP2A-C catalytic subunit (4B7) antibodies, and recombinant PP1 and PP2A catalytic subunit were from Cell Signaling Technology/Ozyme (Saint-Quentin en Yvelines, France). Secondary species-specific antibodies were from Jackson Immunoresearch (West Baltimore Pike, PA). Hyperfilm MP, ECL and alkaline phosphatase reagents were from Amersham Life Sciences (Arlington Heights, IL). Fura-2/AM was from VWR International (Fontenay s/s Bois, France). TransMessenger Transfection Reagent and the QuantiTect SYBR Green PCR Master Mix was from Qiagen (Courtaboeuf, France). The Guava Nexin assay was from Guava Technologies (Hayward, CA). Malachite Green Ser/Thr Phosphatase Assay kit 1 was from Euromedex (Mundolsheim, France).

Cell culture

The human colon carcinoma cell lines HT-29, SW480, LoVo and HCT-116 purchased from the American Type Culture Collection (Manassas, VA) were grown in Dulbecco's Modified Eagle Medium (DMEM) or F12 medium containing L-glutamine (for Lovo cells) supplemented with 10% fetal calf serum (FCS), 100 μg/ml streptomycin and 100 U/ml penicillin. MCF-7 breast carcinoma cells were grown in DMEM supplemented with 10% FCS, 1% L-glutamine and 1% penicillin/streptomycin. MCF-7 cells were stably transfected with 10 μg pcDNA3.0 or with 10 μg pcDNA3.0/caspase 3. Forty-eight hours after transfection cells were grown in medium containing 800 μg/ml G418. After 4 weeks, stable transfectant cells were selected by limiting dilution and designated MCF-7 control cells and MCF-7 Casp-3 cells, respectively. Exposure of MFC-7 Casp-3 to 1 μM staurosporine for 6 h resulted in the induction of caspase 3 activity, and was characterized by the appearance of the ladder nucleosomal DNA fragments characteristic of apoptosis (data not shown).

Cell cycle analysis

HT-29 cells were treated with various concentrations of DPE. After 24 h, the floating and adherent cells were pooled, centrifuged, washed several times with phosphate-buffered saline (PBS) and then fixed with 70% ice-cold ethanol. Pelleted cells were resuspended in RNAse A (180 μg/ml) and incubated at room temperature for 30 min. PI (Merck, Darmstadt, Germany) (50 μg/ml final concentration) was added, and the cells were incubated at room temperature and in the dark for 15 min. PI was excited at 488 nm, and the fluorescence was analyzed at 630 nm. The percentages of $subG_1$; G_0/G_1, S and G_2/M cells were determined by flow cytometry, using an Epics, Elite ESP coulter cytometer (Beckman Coulter, Fullerton, CA) and the Wincycle software program (Beckman Coulter, Fullerton, CA).

Immunoblot analysis

Cells were rinsed, scraped off and collected in ice-cold PBS containing a cocktail of protease and phosphatase inhibitors. Protein concentration was measured by Bio-Rad assay, using bovine serum albumin (BSA) as a standard. Equal amounts of cell protein extract (25 μg) were run on 7 or 10% SDS–PAGE. After being transferred onto nitrocellulose, membranes were blotted with the following primary antibodies diluted in TBS containing 0.1% Tween: rabbit anti-c-jun phospho-specific (dilution 1:2000), anti-SAP/JNK (dilution 1:1000), anti-SAP/JNK phospho-specific (dilution 1:5000), anti-eIF2α (dilution 1:1000), anti-eIF2α phospho-specific (dilution 1:1000),

anti-$Erk_{1/2}$ (dilution 1:1000), anti-$Erk_{1/2}$ phospho-specific (dilution 1:1000), anti-Akt/PKB (dilution 1:1000), anti-Akt/PKB phospho-specific (dilution 1:1000), anti-PERK phospho-specific (dilution 1:1000), anti-GSK3β phospho-specific (dilution 1:5000), anti-Nox-4 (dilution 1:200), anti-IKKβ phospho-specific (dilution 1:500), anti-cleaved caspase 3 antibodies (dilution 1:1000), anti-Bak (dilution 1:500), mouse anti-CHOP/GADD153 (dilution 1:250), anti-GRP78/Bip (dilution 1:1000), anti-Bax (dilution 1:300), anti-Bad phospho-specific (dilution 1:500), anti-c-jun (dilution 1:1000), anti-β-actin (dilution 1:3000), anti-PP2A-C (dilution 1:1000) and anti-Bcl-2 (dilution 1:100) Mabs. After rinsing, the membranes were incubated with an appropriate species-specific secondary peroxidase-conjugated or alkaline phosphatase-conjugated antibodies (dilution 1:20 000 or 1:5000). The membranes were then washed in TBS/0.1% Tween, and proteins were detected using chemiluminescence or alkaline phosphatase detection. The blots were probed using a mouse anti-human β-actin Mab, used as the internal standard. Labeled protein bands were scanned with an HP Scanjet 5500, and the relative protein content was determined by densitometric analysis.

Real-time PCR

HT-29 cells were or were not incubated with 200 μM DPE for 16 h, and the total RNA was extracted by the Nucleospin RNA II kit according to the manufacturer's instructions. Equal amounts of total RNA were reverse-transcribed using random hexamer and Superscript II reverse transcriptase. All the samples for comparison were reverse-transcribed from the same reverse transcription mixture. Expression levels of human XBP-1 and GRP78/Bip mRNAs were measured by quantitative real-time PCR using the specific primers as follows: XBP-1; forward primer 5′-CCGCAGCAGGTGCAGG-3′ and reverse primer 5′-GAGTCAATACCGCCAGAATCCA-3′. The forward primer was designed to span the 26 bp small intron. Thus, this pair of real-time primers can specifically amplify the spliced XBP-1 mRNA transcripts produced by Ire1 activation. GRP78/Bip; forward primer 5′-TCCTGCGTCGGCGTGT-3′ and reverse primer 5′-GTTGCCCTGATCGTTGGC-3′, and β-actin; forward primer 5′-CCTGGCACCCAGCACAAT-3′ and reverse primer 5′-GCCGATCCACACGGAGTACT-3′. The specificity of each of the amplified products generated was confirmed by melting curve analysis and gel electrophoresis. The QuantiTect SYBR Green PCR Master Mix (Qiagen) and the ABI Prism 7700 sequence detection system (Applied Biosystems) were used to detect the real-time quantitative PCR products of reverse-transcribed cDNA samples, according to the manufacturer's instructions. The cycling program conditions were as follows: 95°C for 15 min followed by 40 cycles of 15 s at 94°C, annealing for 30 s at 60°C and extension for 30 s at 72°C. PCRs were performed in triplicate for each experimental condition tested. mRNA expression was quantified by relating the PCR threshold cycle obtained from samples to a cDNA standard curve. The normalized amount of mRNA was obtained by dividing the averaged sample value by the averaged β-actin value.

Small interfering RNA (siRNA)

Experiments were carried out using specific HPP Grade dXdY siRNA (Xeragon-Qiagen), designed by selecting a cDNA target region from the catalytic subunit of PP2A (GenBank accession no. BC000400; 5′-CACCUUUGGGCAAGAUAUU-3′) located 453 bp from the start codon. Scrambled siRNA non-homologous to the human genome was used as a control. To achieve optimal transfection efficiency, various parameters including the amounts of transfection reagent, RNA and TransMessenger–RNA complexes, cell density, and the length of exposure of cells to TransMessenger–RNA complexes were optimized. Twenty-four hours before transfection, HT-29 cells were transferred onto 6-well plates (5×10^5 cells per well) and incubated with 0.8 μg of each siRNA duplex using TransMessenger Transfection Reagent for 4 h in medium devoid of serum and antibiotics. We checked that this procedure did not affect cell viability. Cells were then rinsed with PBS, and grown in complete medium for a further 24 h before gene-silencing experiments.

Transient transfection and luciferase reporter assay

HT-29 cells (8×10^6 cells) were transfected by electroporation with pAP-1-Luc or $p(\kappa B)_3$ IFN-Luc plasmids (Luciferase *cis*-reporter system containing 7× AP-1 and 3× NF-κB enhancer elements, respectively). Electric pulsing (275 V and 955 μF) was applied in the Bio-Rad Gene Pulser. Cells were placed on ice for 15 min and then seeded at 5×10^5 cells/well in 6-well dishes. An empty luciferase plasmid, pLuc-MCS, was used as a control. After transfection, the cells were cultured for 48 h and then treated with 100 ng/ml tumor necrosis factor-α (TNF-α) or with various concentrations of DPE for additional 4 h. The cells were harvested, and the luciferase activities were measured using a luminometer according to manufacturer's instructions.

Intracellular calcium measurement

Intracellular calcium was measured using Fura-2/AM. HT-29 cells (5×10^3 cells/ml) were seeded onto glass cover-slips and then loaded with 5 μM of Fura-2/AM in Na-HEPES-buffered saline (pH 7.4) (135 mM NaCl, 4.6 mM KCl, 1.2 mM $MgCl_2$, 11 mM HEPES, 11 mM glucose and 0.01% pluronic acid) containing or not 1.5 mM $CaCl_2$ for 45–60 min at 37°C. The fluorescence was recorded at 10 s intervals over 10 min in the presence or absence of extracellular Ca^{2+} using a dual-wavelength excitation fluorimeter (excitation: 340 and 380 nm, emission: 510 nm). Recordings were performed on cells incubated with 200 μM DPE alone or with 1 μM thapsigargin.

Apoptotic cell measurement by annexin V labeling

Apoptosis was analyzed using the Guava Nexin kit, which discriminates between apoptotic and non-apoptotic cells. The Guava Nexin assay utilizes annexin V-Phyco-Erythrin (annexin V-PE). A total of 2×10^6 cells were seeded in 60-mm diameter Petri dishes and grown for 24 h in complete culture medium. The medium was then replaced with fresh culture medium containing no or a range of different concentrations of DPE for various times and apoptotic cell staining was performed according to the manufacturer's instructions using the Guava PCA system. Results were expressed as the percentage of apoptotic annexin V-PE positive. When used, the caspase inhibitors Z-VAD-fmk (200 μM) and Z-DEVD-fmk (50 μM), calyculin A (10–100 nM) or okadaic acid (10–1000 nM) were added 1 h before the treatment with DPE.

Transmission electron microscopy

Transmission electron microscopy was performed on HT-29 cells treated or not with 200 μM DPE for 24 h. Samples were fixed for 1 h with 2% glutaraldehyde prepared in a 0.1 M cacodylate buffer solution (pH 7.4), post-fixed in osmium tetroxide, dehydrated with graded ethanol series and finally embedded in Epon. Ultrathin sections were examined in a Jeol JEM-100 CX11 electron microscope operated at 100 kV. ER area was calculated by determining the relative surface density according to the method reported previously (31). Briefly, four independent sets of electromicrographs of control and DPE-treated cells (200 μM) at magnification ×8000 were analyzed. The relative area was equal to twice the number of line intersections with the ER membrane divided by the total length of line on the containing space. The mean cell area (μm^2) was determined in 20 fields.

Flow cytometry analysis

After being counted, the floating and attached cells were pooled. Samples were run on a Becton Dickinson FACScalibur (Immunocytometry Systems, San Jose, CA) equipped with a 15 mW, 488 nm argon laser and filter configuration for FITC/PI dye combination. The quantitative determination of the percentage of cells undergoing apoptosis was performed using the annexin V-FITC Apoptosis Detection kit according to the manufacturer's instructions. The mitochondrial potential was measured using 3,3′-dihexyloxacarbocyanine iodide ($DiOC_6$: 40 nM final concentration, 15 min, 37°C). $DiOC_6$ mitochondrial potential-related fluorescence was immediately recorded by flow cytometry. The green fluorescence was collected through a 524–544 nm band pass filter, and the fluorescent signals were measured on a logarithmic scale of four decades of log. For each sample, data from 10 000 cells was acquired and analyzed using LYSYS I software (Becton Dickinson).

Cytochrome c release and cleaved forms of caspases 3 analyses

HT-29 cells were seeded in 75 cm^2 culture dishes (10^6/dish) and grown in standard culture medium for 24 h. The medium was then replaced by a fresh culture medium with or without DPE, and the cells were grown for a further 24 h. After cell lysis, cytochrome *c* and Cox 4, an integral mitochondrial transmembrane protein, were detected in the cytosol and in mitochondria-enriched fraction by western blotting (10 000× *g* supernatant after centrifuging for 25 min at 4°C) using an Apoalert Cell Fractionation kit according to the manufacturer's instructions.

Detection of cleaved form of caspases 3

Parental and caspase 3-overexpressing MCF-7 cells (7×10^5) were grown for 24 h, and then processed with or without 200 μM DPE in the presence or absence of Z-DEVD-fmk inhibitor. After 24 h, cell lysates were probed with a rabbit polyclonal anti-cleaved caspase 3 antibody, which specifically recognizes cleaved enzyme isoforms.

Phosphatase activity assay

Phosphatase activity was determined using a malachite green phosphatase assay by measuring the dephosphorylation of phosphopeptide substrate R-K-(pT)-I-R-R.

Phosphatase activity assay in cell homogenates. HT-29 cells were incubated with various concentrations of DPE for 1 h, and were then lysed with

phosphatase lysis buffer containing 20 mM HEPES (pH 7.4), 10% glycerol, 0.1% Nonidet P-40 (NP-40), 1 mM EGTA, 0.1 mM $MgCl_2$, 30 mM β-mercaptoethanol, 1 mM phenylmethyl-sulfonyl fluoride (PMSF) and protease inhibitors cocktail. Cells were scraped off and sonicated on ice for three 10 s pulses, and then centrifuged for 5 min at 2000× *g* at 4°C. Aliquots of the supernatant were assayed for protein content using a Bio-Rad assay, with BSA as a standard. Samples were resuspended in buffer containing 50 mM Tris–HCl (pH 7.0), 0.1 mM EDTA with or without 1 μM okadaic acid in the presence of various concentrations of DPE. Reactions were initiated by adding 175 μM phosphopeptide substrate R-K-(pT)-I-R-R to the mixture for 0–15 min. The reaction was terminated by adding 100 μl malachite green detection solution for 15 min. Absorbance was measured at 620 nm and corrected by subtracting the reading for blank wells containing no enzyme. The amount of phosphate released was determined by comparing absorbance with a standard phosphate curve.

In vitro phosphatase activity assay. Ser/Thr phosphatase 1 (PP1) (0.05 U) and PP2A (0.025 U) catalytic subunits were incubated with or without various concentrations of DPE in the presence or absence of 10 nM calyculin A or 10 nM okadaic acid. Phosphatase assay buffer and phosphopeptide R-K-(pT)-I-R-R were added to produce a final volume of 25 μl. Reactions were initiated by adding 175 μM phosphopeptide, and the reaction mixtures were incubated at 37°C for 10 min. Reactions were terminated by adding 100 μl of malachite green solution. Activities of PP1 and PP2A were determined using a spectrophotometer and measuring the absorbance at 620 nm.

Statistical analysis

Results are expressed as mean ± SD from triplicate determinations for 3–4 separate experiments for each set of conditions tested. Significant differences between groups were analyzed by the unpaired Student's *t*-test. A *P*-value of <0.05 was considered significant.

Results

DPE induces cell growth arrest and apoptosis in colon cancer cell lines

The potential action of DPE on cell cycle and cell viability was analyzed by flow cytometry analysis in human colon carcinoma HT-29 cells treated with various concentrations of DPE. DNA flow cytometry analysis revealed that DPE induced a dose–response shift in the cell cycle distribution. HT-29 cells treated with 400 μM DPE for 24 h exhibited higher percentages of cells in the $subG_1$-phase (+DPE: 10.3% ± 1.1; Control: 0.8% ± 0.2), S-phase (+DPE, 31.2% ± 2.9; Control, 23.4% ± 4.0), and G_2/M-phase (+DPE, 20.4% ± 3.8; Control, 9.6% ± 2.1) and a lower percentage of cells in the G_0/G_1-phase (+DPE, 38.1% ± 3.1; Control, 66.2% ± 4.5) than those for the corresponding set of control cells (Figure 1A). These results indicate that DPE caused S-phase and G_2/M-phase arrest thus preventing the cells from entering into mitosis, and induced the appearance of cells with $SubG_1$ DNA content. We next analyzed the action of DPE on cell viability using the annexin V-PE Guava Nexin kit that discriminates between apoptotic and non-apoptotic cells. As shown in Figure 1B, DPE induced cell death in a dose-dependent manner: after incubating for 24 h, the low concentration of DPE (100 μM) had induced ∼20% cell death whereas the highest concentration of DPE (400 μM) had induced ∼65% cell mortality. The percentage of cell death also increased significantly as a function of incubation time. Similar time- and concentration-dependent effects of DPE on cell death were also observed in other carcinoma colon cell lines, such as HCT-116, SW480 and LoVo (Figure 1B, inset). In all cases, the concentration of DPE inducing a 50% cell growth inhibition (IC_{50}) was ∼200 μM (data not shown). HT-29 cells treated with DPE (200–400 μM) for 24 h were then analyzed by flow cytometry analysis, using double labeling with annexin V and PI to quantify the number of apoptotic cells (R1, annexin V^+/PI^-), necrotic cells (R2, annexin V^+/PI^+ cells) and damaged cells (R3, annexin V^-/PI^+) (Figure 1C). Incubating HT-29 with DPE for 24 h led to a significant increase in the percentage of apoptotic cells (32 and 48% of the total cell population at 200 and 400 μM DPE, respectively), and to a lesser extent in the percentage of necrotic cells (10 and 18% of the total cell population for 200 and 400 μM DPE, respectively) and damaged cells (4 and 10% of the total cell population for 200 and 400 μM DPE, respectively). Similar results were obtained on SW480 and HCT116 cells treated with DPE (data not shown). Ultrastructural studies confirmed the inducible apoptotic action of DPE. Nuclei of HT-29 cells treated with 200 μM DPE for 24 h exhibited typical features of apoptosis including chromatin condensation, fragmented nuclei and presence of apoptotic bodies (Figure 1D). These overall findings indicate that DPE induced arrest of cell cycle progression and triggered apoptosis in colon adenocarcinoma cells.

DPE alters mitochondrial membrane permeablization and stimulates caspase 3

Mitochondrial outer membrane permeabilization, which is responsible for a change in the mitochondrial transmembrane potential ($\Delta\psi_m$) and/or release of soluble proteins in the intermembrane space, appears to be closely associated with cell death. We therefore examined the effects of DPE on the transmembrane potential $\Delta\psi_m$ and by measuring cytochrome *c* release. HT-29 cells were incubated without or with 200 or 400 μM DPE for 24 h, and then stained with the cationic lipophilic dye $DiOC_6$. Flow cytometry analysis revealed that DPE altered the pattern of cytosolic fluorescence, with low values of $\Delta\psi_m$ reflecting a loss of mitochondrial potential compared with untreated cells (Figure 2A). Western blot analysis also showed that DPE triggered the release of cytochrome *c* from the mitochondria into the cytosolic fraction of HT-29 cells (Figure 2B). The purity of the cytosol and membrane fractions from untreated or DPE-treated HT-29 cells was confirmed by western blotting using an antibody raised against the integral mitochondrial membrane protein Cox 4 (Figure 2B). We next analyzed the effect of DPE on the expression of anti-apoptotic Bcl-2 and pro-apoptotic Bcl-2 proteins, including Bax, Bak and Bad, which are known to regulate mitochondrial-mediated apoptosis by controlling mitochondrial membrane permeability, and the release of cytochrome *c*. Adding 400 μM DPE to HT-29 cells for 24 h caused a dramatic reduction in protein expression of Bcl-2, and concomitant increases in protein expression of Bax and Bak and activation of the pro-apoptotic Bad protein by reducing its phosphorylated form (Figure 2C). These early apoptotic events are known to induce the activation of downstream proteolytic cascades involving caspases, which cleave specific intracellular substrates and commit the cells to apoptotic death. Inhibition of such proteolytic cascades can be achieved using pan-caspase inhibitor, Z-VAD-fmk. By using an antibody that only recognizes the activated form of caspase 3, we checked that DPE was inducing the activation of caspase 3 (Figure 2D; inset). Furthermore, adding 200 μM Z-VAD-fmk to HT-29 cells incubated with 400 μM DPE for 24 h prevented DPE-induced cell death (Figure 2D). These findings strongly suggest that DPE triggered proteolytic cleavage of the pro-caspase 3 in HT-29 cells. To confirm these results, we used MCF-7 breast carcinoma cells, which harbor a deletion in *caspase 3* gene and lack functional caspase 3, and in MCF-7 cells overexpressing caspase 3. As shown in Figure 2E,

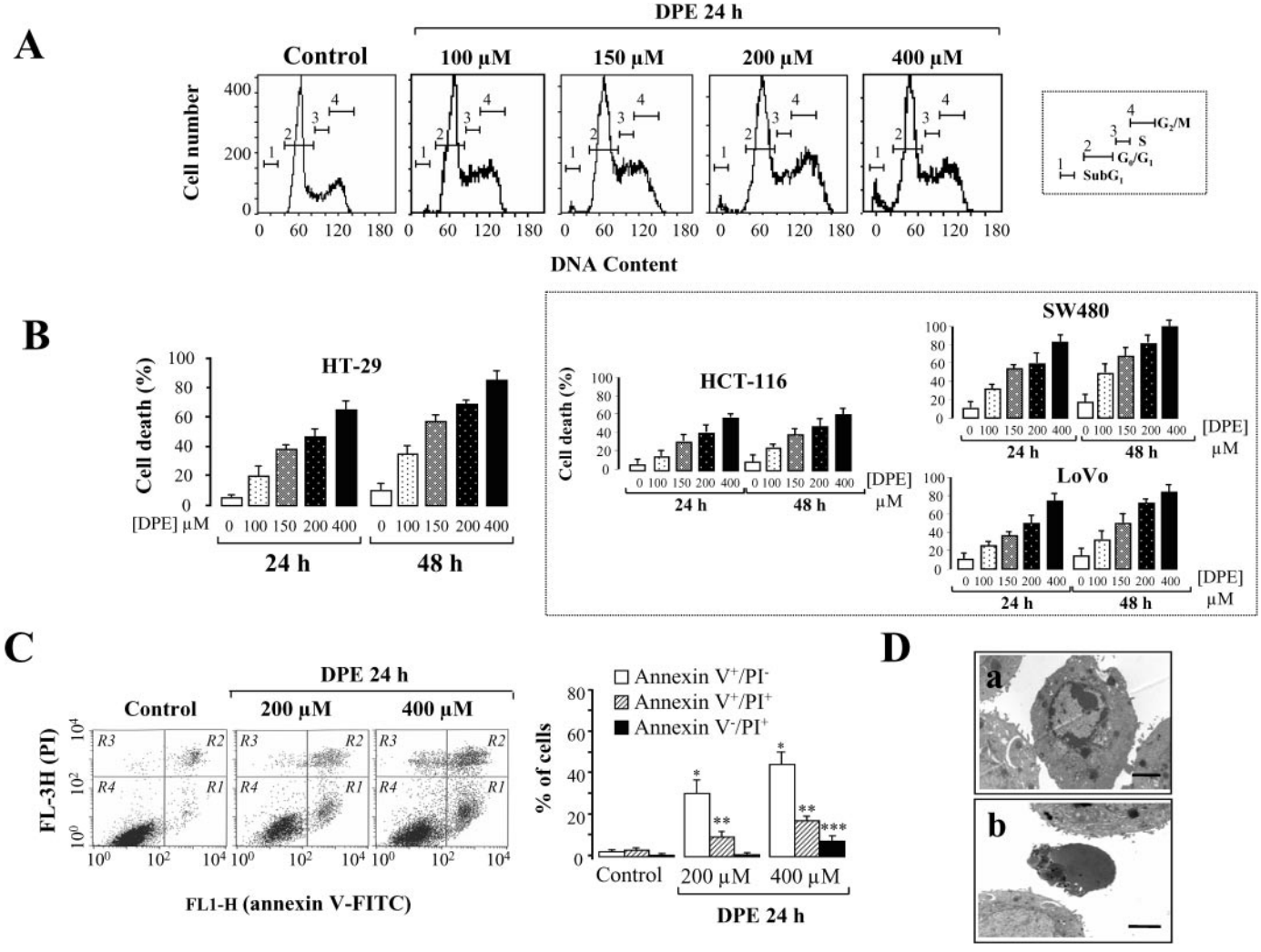

Fig. 1. DPE induces cell cycle arrest and apoptosis in HT-29 cells. (**A**) Cell cycle stage distribution was analyzed by flow cytometry in HT-29 cells processed without 0 (Control) or with 100, 150, 200 or 400 µM DPE for 24 h. The percentage of cells in (i) subG$_1$-; (ii) G$_0$/G$_1$-; (iii) S- and (iv) G$_2$/M-phases was quantified from three different experiments using the Wincycle software program. (**B**) The percentage of cell death was quantified using the Guava Nexin kit (annexin V-PE) in HT-29 cells and in three other colon cancer cell lines (HTC-116, SW480 and LoVo), incubated with various concentrations of DPE for 24 and 48 h, as described in Materials and methods. The bars represent the mean values ± SD of triplicate counts of four separate experiments. (**C**) Flow cytometry analyses were performed on HT-29 cells incubated without (Control) or with 200 and 400 µM DPE for 24 h. The illustrations of the plots of annexin V versus PI fluorescence are representative of three separate experiments. R1, apoptotic cells (annexin V$^+$/PI$^-$); R2, necrotic cells (annexin V$^+$/PI$^+$); R3, damaged cells (annexin V$^-$/PI$^+$); R4, viable cells (annexin V$^-$/PI$^-$). The bars represent the percentage of annexin V$^+$/PI$^-$, annexin V$^+$/PI$^+$ and annexin V$^-$/PI$^+$ cells after exposure to 0 (Control), 200 or 400 µM of DPE for 24 h. The bars represent the mean values ± SD from three separate experiments. $^*P < 0.001$; $^{**}P < 0.01$; $^{***}P < 0.05$ versus control values for each experimental condition tested. (**D**) Illustrations of different morphological states of apoptosis showing (a), peripheral chromatin condensation and (b), formation of apoptotic bodies in HT-29 cells incubated with 200 µM DPE for 24 h. Bar, 5 µm.

DPE did not induced cell death in MCF-7 cells transfected with an empty vector but did significantly induce cell death in MCF7 cells overexpressing caspase 3 (Figure 2E). This apoptotic effect of DPE was reduced to some degree when MCF-7 cells overexpressing caspase 3 were treated with 50 µM Z-DEVD-fmk, a specific caspase 3-inhibitor (Figure 2E).

DPE disturbs ER Ca^{2+} homeostasis

Several non-mutually exclusive pathways have been shown to be involved in the induction of cell apoptosis. The experiments described above have provided several lines of evidence that DPE triggers an intrinsic pathway characterized by disruption of the mitochondrial potential and release of cytochrome *c*. Because the ER has been shown to be involved in apoptotic execution due to an imbalance between pro-apoptotic and anti-apoptotic molecules operating at the ER, we hypothesized that DPE may also induce prolonged ER stress, which in turn activates the UPR and causes cells to undergo apoptosis. To test this hypothesis, experiments were undertaken to determine whether DPE activates specific stress response pathways in colon carcinoma HT-29 cells. The maintenance of Ca^{2+} homeostasis within the ER is essential for many cellular functions, including protein folding, processing, transport and signal transduction. Perturbation of ER Ca^{2+} homeostasis is one of the early events leading to disruption of ER functions. Incubating HT-29 cells with 200 µM DPE led to a rapid but transient increase in intracellular $[Ca^{2+}]_i$ independently of the presence of extracellular Ca^{2+} (Figure 3A). The rise in $[Ca^{2+}]_i$ was prevented in cells pre-treated with 1 µM thapsigargin, which depletes Ca^{2+} intracellular stores by inhibiting

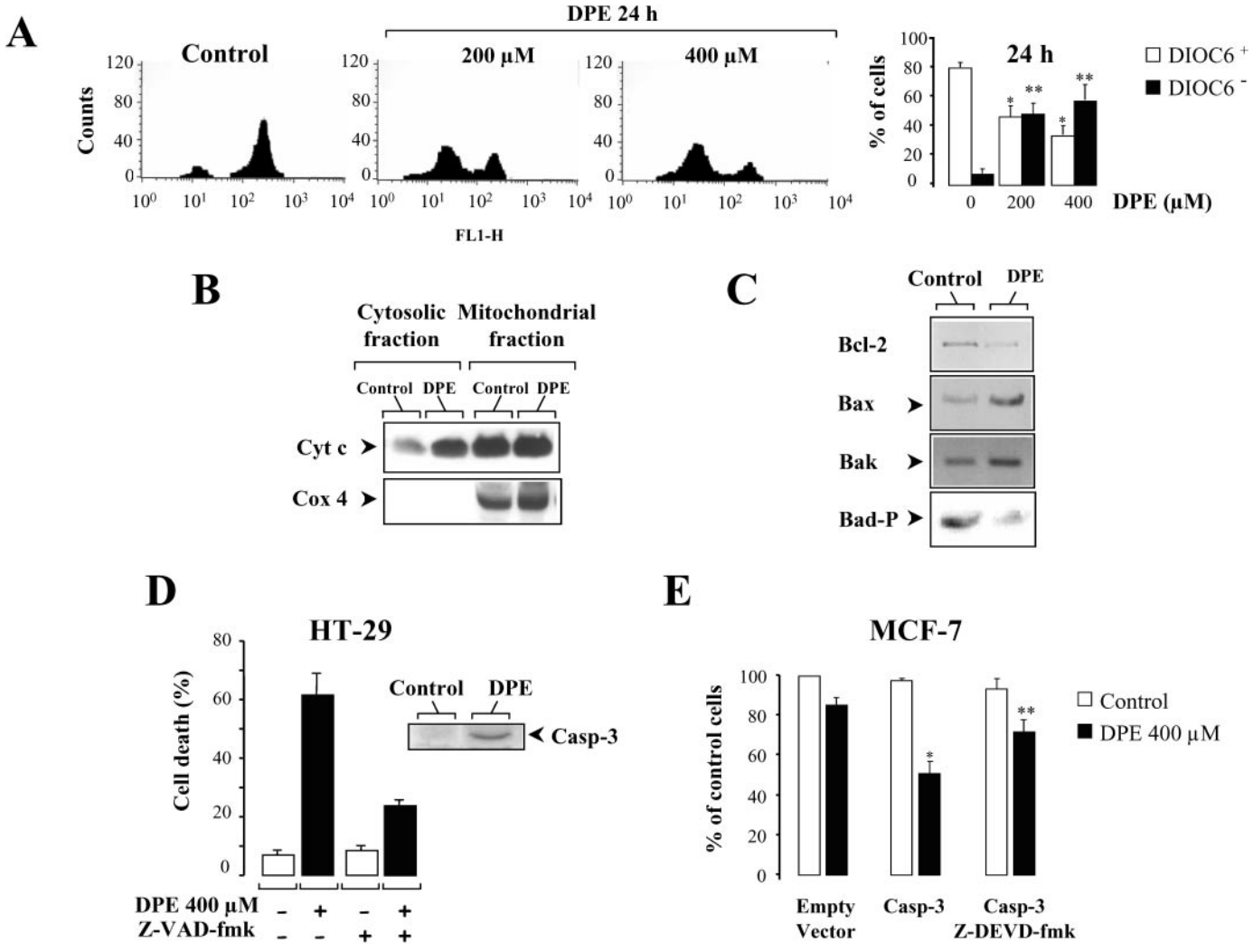

Fig. 2. DPE induces cytochrome *c* release from the mitochondria and caspase 3 activation. (**A**) HT-29 cells were incubated without (Control) or with 200 or 400 µM DPE for 24 h. The percentage of cells with low mitochondrial potential was determined by flow cytometry with $DiOC_6$. The bars represent the mean values ± SD of five separate experiments. $^{*}P < 0.01$; $^{**}P < 0.05$ versus control cell values. (**B**) HT-29 cells were treated without (Control) or with 400 µM DPE (DPE) for 24 h. The release of cytochrome *c* from the mitochondria was determined on cytosolic and mitochondrial fractions separated by subcellular fractionation and analyzed by western blotting (10 µg of each fractions) using antibodies directed against cytochrome *c* (Cyt c) and Cox 4, a transmembrane marker of mitochondria. The western blots shown are representative of three separate experiments. (**C**) Lysates of HT-29 cells incubated without (Control) or with 400 µM DPE (DPE) for 24 h were immunoblotted (100 µg of protein loaded) for anti-apoptotic Bcl-2, pro-apoptotic Bax, Bak or the phosphorylated form of Bad (Bad-P). The western blots shown are representative of three separate experiments. (**D**) The percentage of cell death was analyzed by the Guava Nexin kit on HT-29 cells incubated without (−) or with 400 µM DPE (+) in the presence (+) or absence (−) of the pan-caspase inhibitor Z-VAD-fmk (200 µM) for 24 h. The bars represent the mean values ± SD of triplicate counts of four separate experiments. (D, inset) Caspase 3 activation was analyzed by western blotting using an antibody directed against the activated form of caspase 3 (Casp-3). (**E**) The implication of the caspase 3 in DPE-induced cell death was analyzed by the Guava Nexin kit on MCF-7 cells transfected with an empty vector or with a human caspase 3 (Casp-3) vector and incubated without (Control) or with 400 µM DPE in the presence or absence of the specific caspase 3 inhibitor, Z-DEVD-fmk (50 µM) for 24 h. The bars represent the mean values ± SD of triplicate counts of four separate experiments. $^{*}P < 0.001$; $^{**}P < 0.01$ versus empty vector-transfected cell values.

sarcoplasmic/endoplasmic reticulum Ca^{2+}-ATPase (SERCA) (Figure 3A). Ultrastructural analyses also revealed that DPE (200 µM for 16 h) caused dramatic swelling and dilatation of the ER from HT-29 cells (Figure 3B; left panel). The semi-quantitative measurements of the ER surface area revealed that DPE caused a significant 3-fold increase of the ER membrane surface areas as compared with untreated cells (Figure 3B; right panel).

DPE induces ER stress in colon cancer cells

Activation of ER stress triggers an UPR response, which includes the induction of genes encoding for ER-resident stress proteins and the attenuation of initiation of protein synthesis. Experiments were undertaken to analyze in detail the effects of DPE on different key regulatory genes encoding for proteins of the UPR.

DPE upregulates XBP-1/GRP78/Bip expression. The *Ire1* gene encodes a type 1 transmembrane Ser/Thr receptor protein kinase, which possesses site-specific endoribonuclease activity. Activated Ire1 mediates frame switching splicing of the bZIP transcription factor XBP-1 mRNA which results in the formation of a potent transactivator that upregulates its own expression and that of molecular chaperones such as

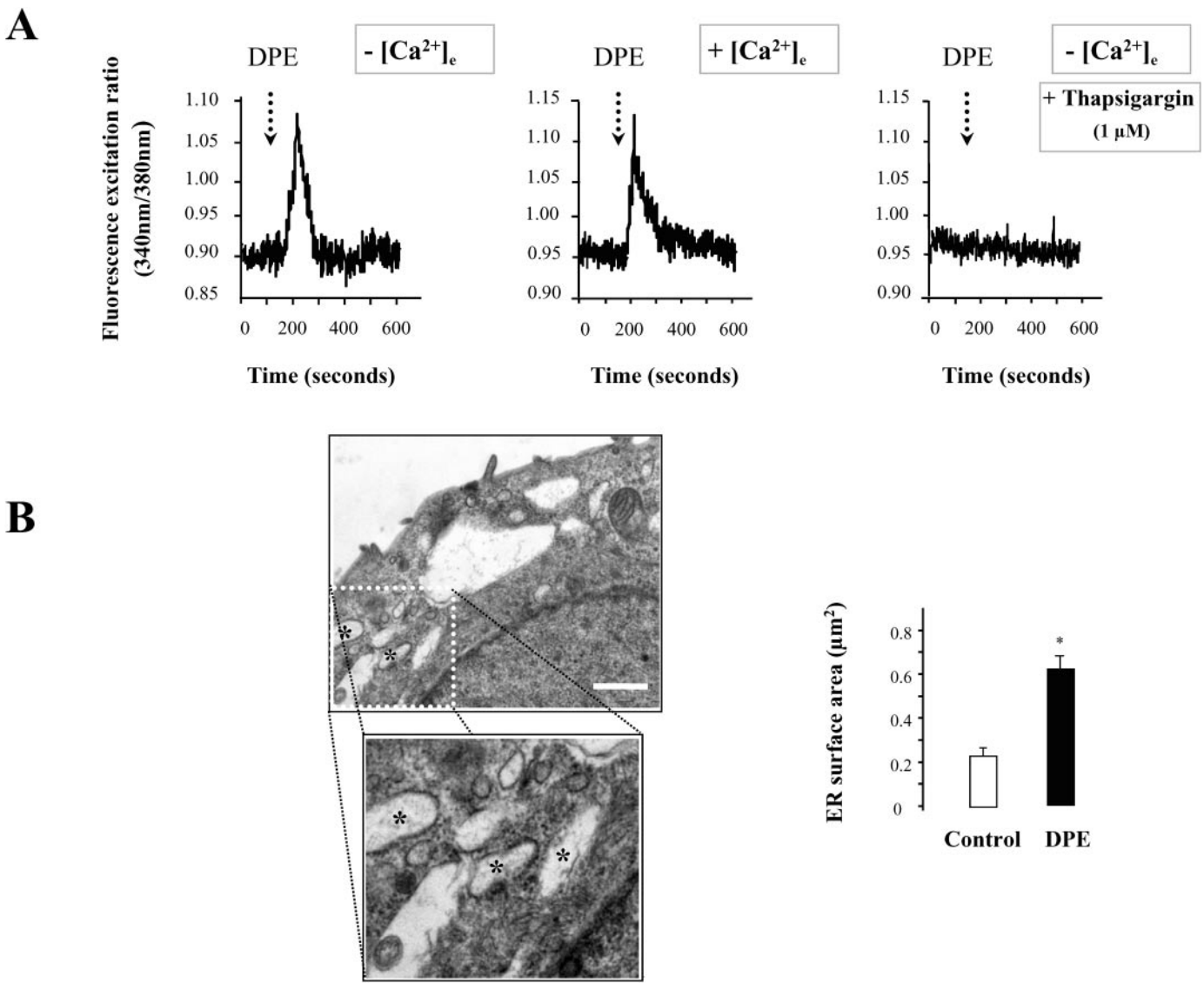

Fig. 3. DPE disturbs ER $[Ca^{2+}]_i$ homeostasis. (**A**) HT-29 cells were loaded with Fluo-2/AM (5 µM for 1 h at 37°C) and 200 µM DPE was added 120 s after the start of the experiment. The emission of fluorescence was recorded for 600 s in the presence ($+[Ca^{2+}]_e$) or absence ($-[Ca^{2+}]_e$) of extracellular Ca^{2+}. When used, 1 µM thapsigargin, a depleting agent of $[Ca^{2+}]_i$ stores, was added at the start of experiment. (**B**) Illustrations (left panels) of ER swelling in HT-29 cells incubated with 200 µM DPE for 24 h. Bar, 1 µm. Asterisk (*) indicate swelling and dilatation of the ER. The bars represent the mean values of ER cell surface area, expressed as μm^2 ± SD counted of 20 different fields of electron micrographs as described in Materials and methods. $^*P < 0.05$ versus control values.

GRP78/Bip. To determine whether DPE activated the Ire1/XBP-1/GRP78/Bip pathway, HT-29 cells were incubated without or with 400 µM DPE for 16 h. Real-time RT–PCR, using primers that specifically amplified only the spliced form of the XBP-1 transcript, showed that the form of XBP-1 associated with Ire1-catalyzed splicing was greatly increased after DPE treatment, whereas it was undetectable in untreated cells (Figure 4A). Consistent with this finding, results from real-time PCR and western blotting revealed that DPE also stimulated in a time-dependent manner the expression of chaperone GRP78/Bip at both mRNA and protein levels (Figure 4A and B).

DPE activates PERK and eIF2α. The pancreatic ER kinase or PKR-like ER-associated kinase (PERK) is an ER transmembrane protein kinase that phosphorylates the subunit of translation initiation factor-2 (eIF2α) responsible for translational attenuation of global protein synthesis in response to ER stress. The phosphorylation status of PERK and eIF2α is therefore a key indicator in ER stress. The time course of the phosphorylation of PERK and eIF2α was analyzed in HT-29 cells treated with 400 µM DPE for various times using phospho-specific antibodies. DPE induced time-dependent changes in the phosphorylation of PERK and eIF2α that were characterized by successive steps of increase and decrease in phosphorylation states, while the protein content of total eIF2α remained unchanged (Figure 4C). The highest levels of phosphorylated PERK and eIF2α were achieved after exposure to DPE for 2 h. These data indicated that DPE activates both main branches of the UPR corresponding to the XBP-1/GRP78/Bip arm downstream to Ire1 and ATF6 ER stress sensors, and the PERK/eIF2α phosphorylation-dependent arm.

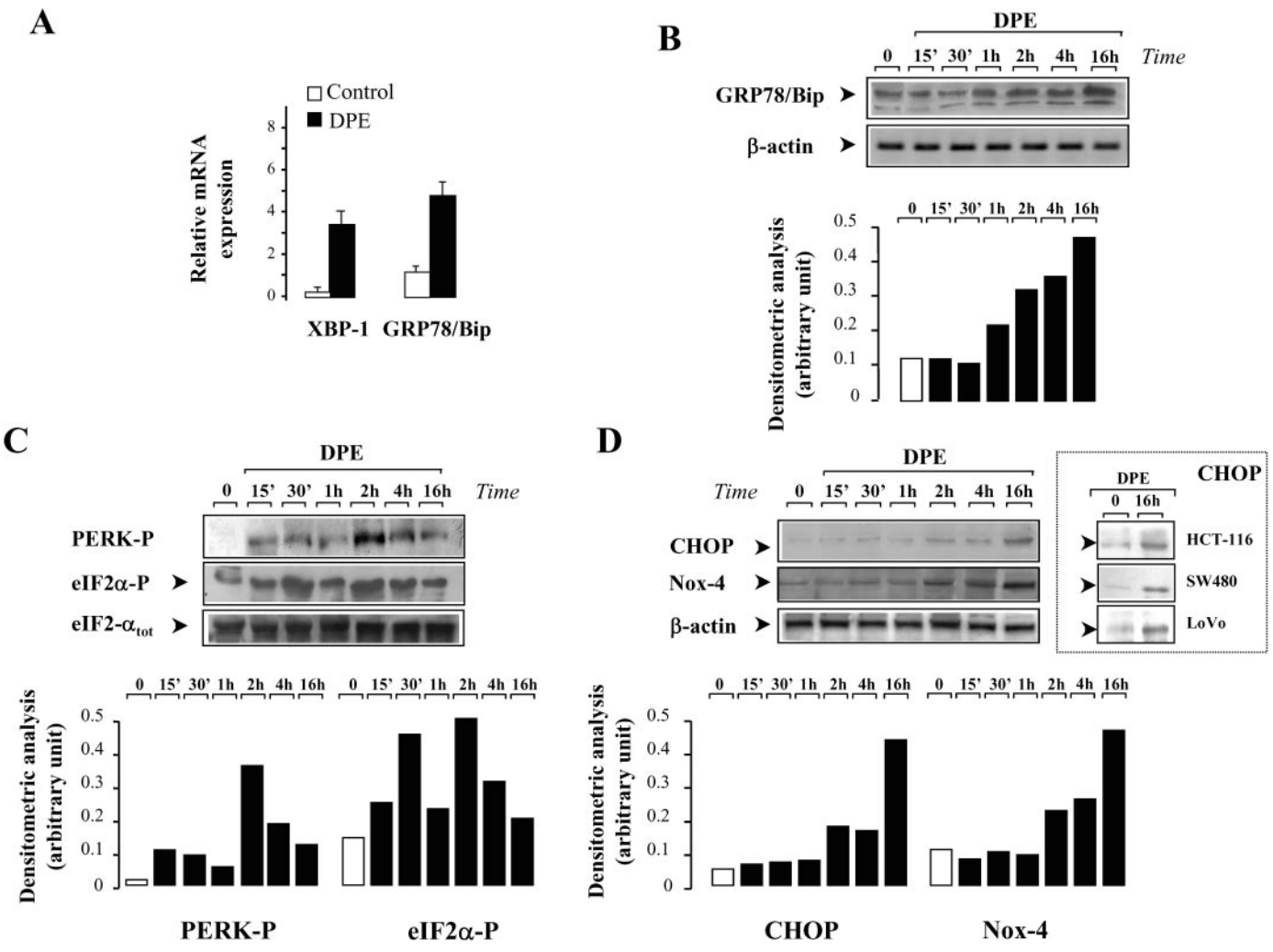

Fig. 4. DPE stimulates ER stress-associated genes in HT-29 cells. (**A**) The mRNA level of XBP-1 (spliced form) and GRP78/Bip were determined by real-time RT–PCR on HT-29 cells processed without (Control) or with 400 μM DPE (DPE) for 16 h. The bars represent the mean values ± SD of three separate experiments. (**B**) Cell lysates from HT-29 cells were incubated without (time 0) or with 400 μM DPE for 15 min (15′) to 16 h and were then immunoblotted for GRP78/Bip. The relative protein content of samples was determined using anti-β-actin antibody as internal standard. (**C**) Western blot analyses using anti-PERK phospho-specific Thr^{980} (PERK-P), anti-eIF2α phospho-specific Ser^{51} (eIF2α-P) and anti-eIF2α (eIF2α$_{tot}$) antibodies were performed on HT-29 cells incubated without (time 0) or with 400 μM DPE for 15 min (15′) to 16 h. (**D**) HT-29 cells were incubated without (0) or with 400 μM DPE for 15 min (15′) to 16 h. Cells lysates were analyzed by western blotting using antibodies directed against CHOP/GAD153 (CHOP), Nox-4 and β-actin. (D, inset), HCT-116, SW480 and LoVo cells were incubated without (0) or with 400 μM DPE for 16 h and CHOP expression was detected by western blotting. In all cases, the bars represent the mean values of densitometric values measured for each experimental condition in three separate experiments.

DPE upregulates CHOP/GADD153 expression. CHOP/GADD153 is the only UPR target that has been shown to be regulated by both the main branches of the UPR. This suggest that cross-talk occurs between ATF6 and Ire1/XBP-1-dependent and PERK-dependent branches (32). CHOP plays an important role in inducing ER stress-mediated apoptosis by downregulating the expression of anti-apoptotic Bcl-2, and by stimulating the production of ROS (33). Here, we show that the basal CHOP expression, which was undetectable in untreated HT-29 cells, gradually increased in DPE-treated cells up to 16 h (Figure 4D), and remained elevated until 48 h (data not shown). Upregulation of CHOP expression was also observed after treatment with DPE for 16 h in other carcinoma colon cell lines, such as HCT-116, SW480 and LoVo (Figure 4D, inset). These data provide additional evidence that cytotoxic concentrations of DPE can activate cellular stress response pathways, including apoptosis in colon carcinoma cells.

DPE upregulates Nox-4 expression. We have recently shown that the non-phagocytic NAD(P)H oxidase homolog Nox-4 plays a key role in the control of ER stress-mediated apoptosis induced by 7-ketocholesterol in human smooth muscle cells (34). 7-Ketocholesterol promotes Nox-4 expression by stimulating the Ire1/JNK/AP-1 signaling pathway, which in turn modulates the expression of CHOP (34). These findings led us to test whether DPE stimulated the expression of Nox-4 in HT-29 cells. DPE (400 μM) induced time-dependent stimulation of the expression of the Nox-4 protein (Figure 4D), which was detectable after 2 h and peaked after 16 h (Figure 4D). These findings indicate that Nox-4, which has previously been shown to be involved in

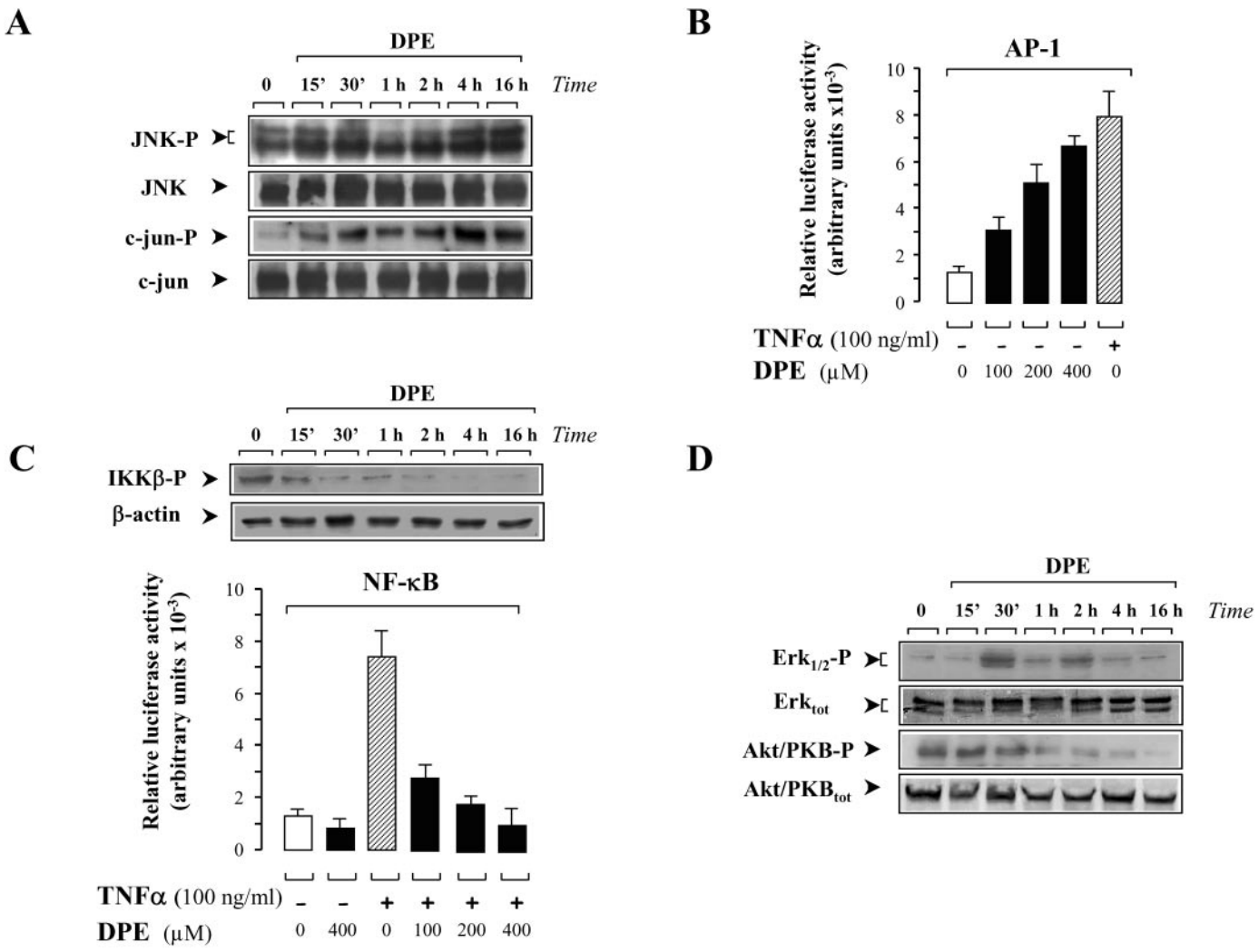

Fig. 5. DPE modulates JNK, $Erk_{1/2}$ and Akt/PKB signaling pathways and the transcriptional activation of the AP-1 and NF-κB promoters. (**A**) Western blot analyses using anti-JNK phospho-specific Thr^{183} and Tyr^{185} (JNK-P), anti-JNK (JNK_{tot}), anti-c-jun phospho-specific Ser^{73} (c-jun-P) and anti-c-jun ($c\text{-}jun_{tot}$) antibodies were performed on HT-29 cells treated without (time 0) or with 400 μM DPE for 15 min (15′) to 16 h. The western blots shown are representative of three separate experiments. (**B**) HT-29 cells were transiently transfected either with an empty luciferase plasmid pLuc-MCS (white bar) or with a plasmid expressing the luciferase *cis*-reporter AP-1. Luciferase activities were measured after exposure for 4 h to the indicated concentrations of DPE. TNF-α (100 ng/ml) was used as a positive control. The bars are mean ± SD of relative luminescence intensity values from three separate experiments performed in triplicate. (**C**) The expression of the phosphorylated form of IKKβ (IKKβ-P) was analyzed by western blotting (upper panel) on HT-29 cells incubated without (time 0) or with 400 μM DPE for 15 min (15′) to 16 h in the presence of TNF-α (100 ng/ml). The same amount of proteins were loaded and checked using an antibody raised against β-actin. The western blots shown are representative of three separate experiments. HT-29 cells were transiently transfected either with an empty luciferase plasmid pLuc-MCS (white bar) or with a plasmid expressing the luciferase *cis*-reporter NF-κB (lower panel). Luciferase activities were then measured after exposure for 4 h to the indicated concentrations of DPE. TNF-α (100 ng/ml) was used as a positive control or in combination with DPE. The bars are mean ± SD of relative luminescence intensity values from three separate experiments performed in triplicate. (**D**) Western blot analyses using anti-$Erk_{1/2}$ phospho-specific Thr^{202} and Tyr^{204} ($Erk_{1/2}$-P), anti-$Erk_{1/2}$ (Erk_{tot}), anti-Akt/PKB phospho-specific Ser^{473} (Akt/PKB-P) and anti-Akt/PKB (Akt/PKB_{tot}) antibodies were performed on HT-29 cells incubated without (time 0) or with 400 μM DPE for 15 min (15′) to 16 h. The western blots shown are representative of three separate experiments.

ER stress-mediated apoptosis, is also upregulated by DPE in HT-29 cells.

DPE activates c-Jun NH_2-terminal kinase and AP-1 transcription factor

Another apoptotic pathway in ER stress involves the activation of the JNK pathway by interacting with Ire1 and TNF receptor-associated factor 2 (TRAF2) (6). Sustained activation of the JNK pathway requires activation of apoptosis signal-regulating kinase (ASK1) by the Ire1/TRAF2 complex, and leads to cell apoptosis via the translocation of the pro-apoptotic factor Bax into the mitochondria (35,36). To investigate the effect of DPE on the ER stress-dependent JNK activation, we first performed western blot analysis on cell homogenates derived from HT-29 cells processed with or without 400 μM DPE for various times using phospho-specific anti-JNK and anti-c-jun antibodies (Figure 5A). While the relative amounts of total JNK and c-jun were not affected by DPE, the levels of phospho JNK and -c-jun proteins increased rapidly under DPE treatment up to 16 h (Figure 5A). Interestingly, two major waves of increasing phosphorylated JNK and c-jun were observed after 30 min and 4 h incubation times with DPE (Figure 5A). To find out whether DPE could modulate AP-1 activity, which is known to be

triggered by JNK phosphorylation and concomitant upregulation of c-fos/c-jun, HT-29 cells were transiently transfected with an AP-1-driven luciferase reporter gene, and then exposed to various concentrations of DPE for 4 h. As shown in Figure 5B, DPE induced a dose-dependent increase in AP-1 transcriptional activity, comparable with those of the TNF-α treated cells used as a positive control.

DPE inhibits TNF-α-induced NF-κB activity

NF-κB activation induced by ER stress requires the release of Ca^{2+} and ROS from the ER as a result of the overloading of the ER with accumulated proteins, and is known as the EOR (5). Conversely, it has been suggested that activation of NF-κB may be involved in the downregulation of the pro-apoptotic JNK pathway (1). To determine whether DPE modulates the transcriptional activity of NF-κB, HT-29 cells were transiently transfected with a NF-κB promoter linked to a luciferase reporter gene construct, and were treated with various concentrations of DPE for 4 h. TNF-α (100 ng/ml), a potent activator of NF-κB activity, strongly stimulated luciferase activity whereas DPE alone (400 μM) failed to stimulate NF-κB transcriptional activity (Figure 5C, lower panel). In sharp contrast, DPE produced dose-dependent downregulation of TNF-α-induced NF-κB activation (Figure 5C, lower panel). NF-κB is regulated primarily by the phosphorylation of the inhibitory proteins, IκBs, which are what retains it in the cytoplasm (37). In response to TNF-α or others agonists, the IκBs are phosphorylated by the IκB kinase (IKK) complex, resulting in their ubiquitination and subsequent degradation, inducing the nuclear translocation of the NF-κB (38). To confirm whether the inhibition of the TNF-α-induced NF-κB activation by DPE resulted from the inhibition of IKK activity, the expression of phosphorylated IKKβ was analyzed by western blotting of untreated- and DPE-treated HT-29 cells in the presence of TNF-α (Figure 5C, upper panel). The results revealed that the TNF-α-induced IKKβ phosphorylation activation was impaired in the presence of DPE. IKKβ dephosphorylation started within 15 min after DPE treatment, and was almost complete within 1–16 h, suggesting that DPE did indeed prevent the TNF-α-induced NF-κB activation by inhibiting IKK phosphorylation.

Effect of DPE on $Erk_{1/2}$ and Akt/PKB signaling pathways

The phosphoinositide-3-kinase (PI3kinase)/Akt-dependent activation of protein kinase B (Akt/PKB) and extracellular sigal-regulated kinase 1/2 ($Erk_{1/2}$) pathways, two well-known pro-survival pathways, have recently been shown to counteract ER stress-induced cell death (39). To test whether DPE affected the activity of $Erk_{1/2}$ and Akt/PKB kinases, cell homogenates derived from HT-29 cells which had been treated with 400 μM DPE at different times were immunoblotted with specific antibodies of phosphorylated forms of $Erk_{1/2}$ and Akt/PKB. As shown in Figure 5D, DPE induced an early and transient peak of $Erk_{1/2}$ phosphorylation within 30 min of incubation, and this was followed by a second, less intense and transient $Erk_{1/2}$ phosphorylation peak after 2 h. In parallel, DPE almost completely abolished the phosphorylation of Akt/PKB within 30 min (Figure 5D). Taken together, these results demonstrate that DPE induces a transient phosphorylation–dephosphorylation of $Erk_{1/2}$ and downregulates the pro-survival Akt/PKB pathway.

DPE activates PP2A activity

The dynamic balance between protein kinase and phosphatase activities toward key substrates has been shown to be crucial for cellular homeostasis. The time-dependent changes in phosphorylation observed in the different signaling pathways induced by DPE suggest that phosphatases may be involved. The major cellular proteins PP1 and PP2A have been shown to be implicated in regulating a broad spectrum of protein kinases and substrates including Akt/PKB, $Erk_{1/2}$, IKK, eIF2α and JNK. One approach to evaluating the role of PP1 and PP2A in regulating cell death induced by DPE was to examine the effect of two potent protein phosphatase inhibitors, calyculin A and okadaic acid. Calyculin A or okadaic acid induced dose-dependent impairment of the HT-29 cell death caused by DPE by up to 64% for 100 nM calyculin A and up to 62% for 1 μM okadaic acid (Figure 6A). Similar cytoprotective effects of protein phosphatase inhibitors were observed in HTC-116, SW480 and LoVo colon carcinoma cells (Figure 6A, inset). Although the selectivity of these inhibitors is not sufficient to discriminate between the respective phosphatase activities of PP1 and PP2A, it is known that calyculin A displays nearly equivalent inhibitory activities against PP1 and PP2A at concentrations of >10 nM, whereas okadaic acid displays 100-fold greater selectivity for PP2A over PP1 at the concentrations used. Furthermore, treatment with calyculin A at 10 nM, a concentration that blocks PP1 but not PP2A, did not significantly protect cells against DPE-induced cell death (Figure 6A), suggesting the preferential role for PP2A in the cytoprotective effect mediated by phosphatase inhibitors. To determine whether DPE promotes an increase in PP2A activity, PP2A activity was measured in cell homogenates derived from HT-29 cells that had or had not been exposed to various concentrations of DPE for 1 h. As shown in Figure 6B, DPE induced a significant increase in Ser/Thr protein phosphatase activity in a time-dependent manner. Adding 1 μM okadaic acid inhibited the phosphatase activity in DPE-stimulated cell homogenates by 67%. Furthermore, DPE stimulated the PP2A activity in a dose-dependent manner with an activity of 2180 ± 95 pmol.mg.cell protein^{-1}.min^{-1} with 400 μM DPE (Figure 6C; lower panel). Immunoblot analysis of cell homogenates using an antibody directed against the catalytic subunit of PP2A (PP2A-C) showed that DPE did not significantly promote any change in PP2A-C levels in tested cell extracts (Figure 6C; upper panel).

To determine whether DPE interacts directly with PP2A, *in vitro* assays were conducted in the presence or absence of a range of concentrations of DPE using the recombinant PP2A catalytic subunit (PP2A-C). The relative phosphatase activity was measured for 10 min by measuring the absorbance at 620 nm, which reflects the phosphate release from synthetic phosphopeptide substrate. As shown in Figure 6D (left panel), DPE increased PP2A activity in a dose-dependent manner, which was specifically blocked by the presence of 10 nM okadaic acid. A similar inhibitory effect was observed with 1 nM okadaic acid (data not shown). To check that DPE acted directly on PP2A activity, but not on PP1 activity, the phosphatase activity of the recombinant PP1 catalytic subunit was measured using synthetic phosphopeptide substrate in the presence or absence of 400 μM DPE. Consistent with the dissociated effects of low concentrations (10 nM) of calyculin A and okadaic acid on the inhibition of DPE-induced cell death, DPE did not affect the calyculin A-sensitive PP1 activity

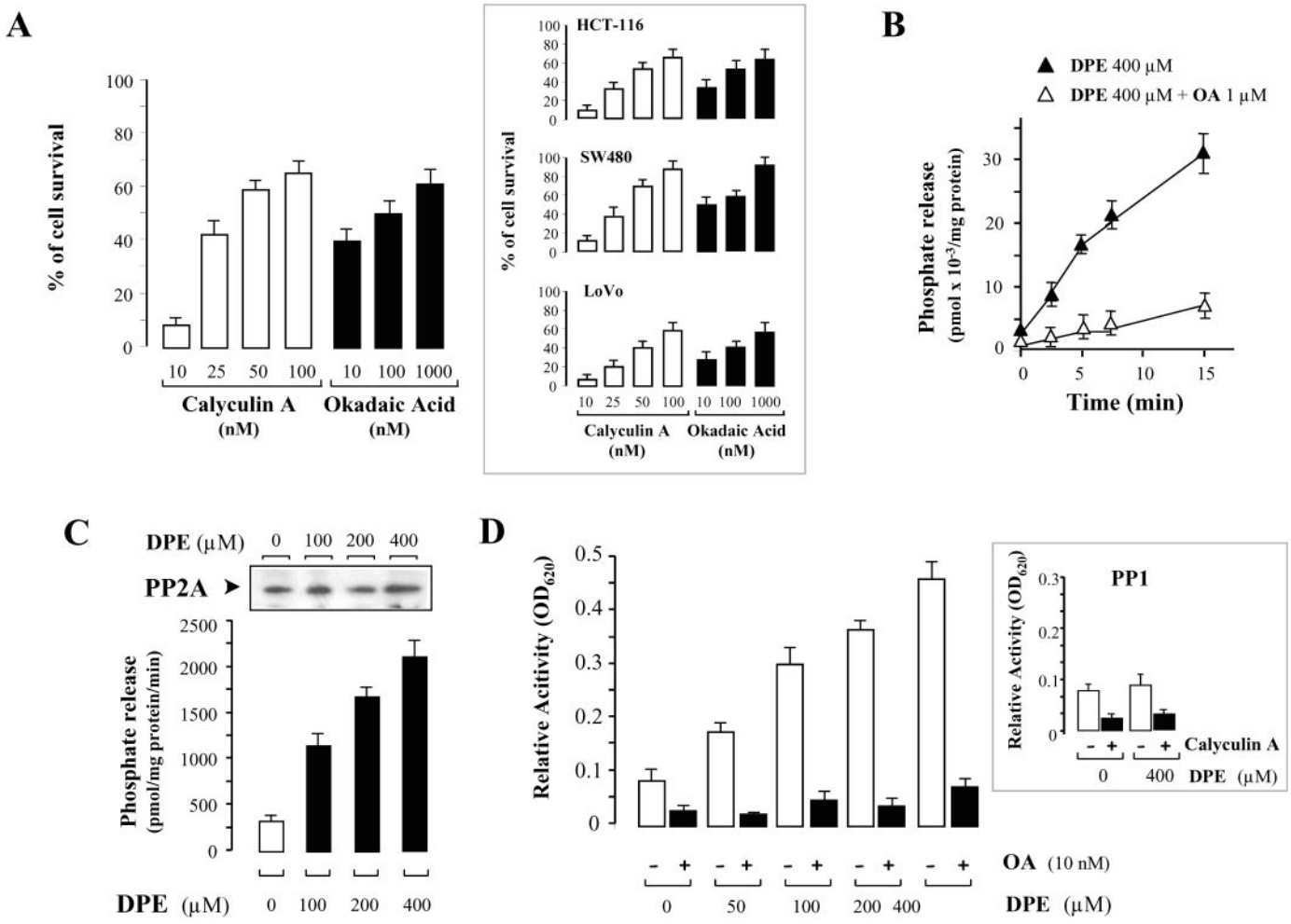

Fig. 6. DPE activates the PP2A activity. (**A**) HT-29 cells and three other colon cancer cell lines (inset) were incubated with 400 μM DPE in the presence of various concentrations of calyculin A or okadaic acid for 24 h. The percentage inhibition of DPE-induced cell death was determined using the Guava Nexin kit, as described in Materials and methods. The bars represent the mean value ± SD of three separate experiments. (**B**) HT-29 cells were treated with 400 μM DPE for 1 h, and the Ser/Thr phosphatase activity was measured in cell homogenates using a synthetic phosphopeptide substrate in the presence or absence of 1 μM okadaic acid (OA) for the times indicated. The bars represent the mean phosphate release value ± SD of triplicate determinations from three separate experiments. (**C**) HT-29 cells were treated without (0) or with increasing concentrations of DPE for 1 h. Cell homogenates were prepared, and the Ser/Thr phosphatase activity (lower panel) was determined using a synthetic phosphopeptide substrate after 15 min recording. The bars represent the mean phosphate release values ± SD of triplicate measurements from three separate experiments. The amount of PP2A protein in the different cell homogenates was detected by western blotting using an antibody directed against the catalytic subunit of PP2A (upper panel). The western blots shown are representative of three separate experiments. (**D**) Ser/Thr protein phosphatase assay using the recombinant PP2A-C (left panel) or PP1-C (right panel) catalytic subunits. The relative phosphatase activity was determined by measuring the optical density at 620 nm (OD_{620}) after incubating for 10 min in the presence or absence of a range of concentrations of DPE, and with or without 10 nM okadaic acid (PP2A-C) or 10 nM calyculin A (PP1-C). The bars represent the mean relative phosphatase activity ± SD of triplicate measurements from three separate experiments.

(Figure 6D; right panel). These findings provide strong evidence that DPE specifically enhanced PP2A activity.

The predominant forms of PP2A are dimers (core enzyme) of catalytic (C) and scaffolding (A) subunits and trimers (holoenzyme) with additional variable regulatory subunits (B, B′, B″), which determine the substrate specificity and localization of the holoenzyme (40). Most PP2A-C subunits in the cell form heterotrimeric complexes, followed in frequency by the PP2A-A and -C core dimers (41–43). To define the possible involvement of PP2A in the DPE-induced cell death, we tested the consequences of downregulating PP2A by RNA interference with cell viability. We chose to target the catalytic C subunit of the phosphatase using small interfering RNA (siRNAs) duplexes to silence PP2A expression. The percentage of cell death was analyzed on scrambled and PP2A-C siRNA-transfected HT-29 cells incubated with or without a range of different concentrations of DPE. As shown in Figure 7A, DPE led to a dramatic increase in the percentage of apoptotic cells in scrambled siRNA-transfected cells. The percentage of cell death in scrambled siRNA-transfected cells was similar to that in untransfected HT-29 cells (see Figure 1B). In contrast, the percentage of apoptotic cells among PP2A-C siRNA-transfected cells treated with 400 μM DPE was 72–75% lower than that among DPE-treated scrambled siRNA-transfected (Figure 7A) demonstrating that DPE-induced cell death was prevented by PP2A silencing. To further validate the silencing effect of PP2A, the amount of PP2A-C protein present in scrambled or PP2A-C siRNA-transfected cells was analyzed by western blotting using the PP2A-C antibody. Consistent with the loss of sensitivity to DPE, the amount of PP2A-C protein was dramatically lower in PP2A-C siRNA-transfected cells than in scrambled

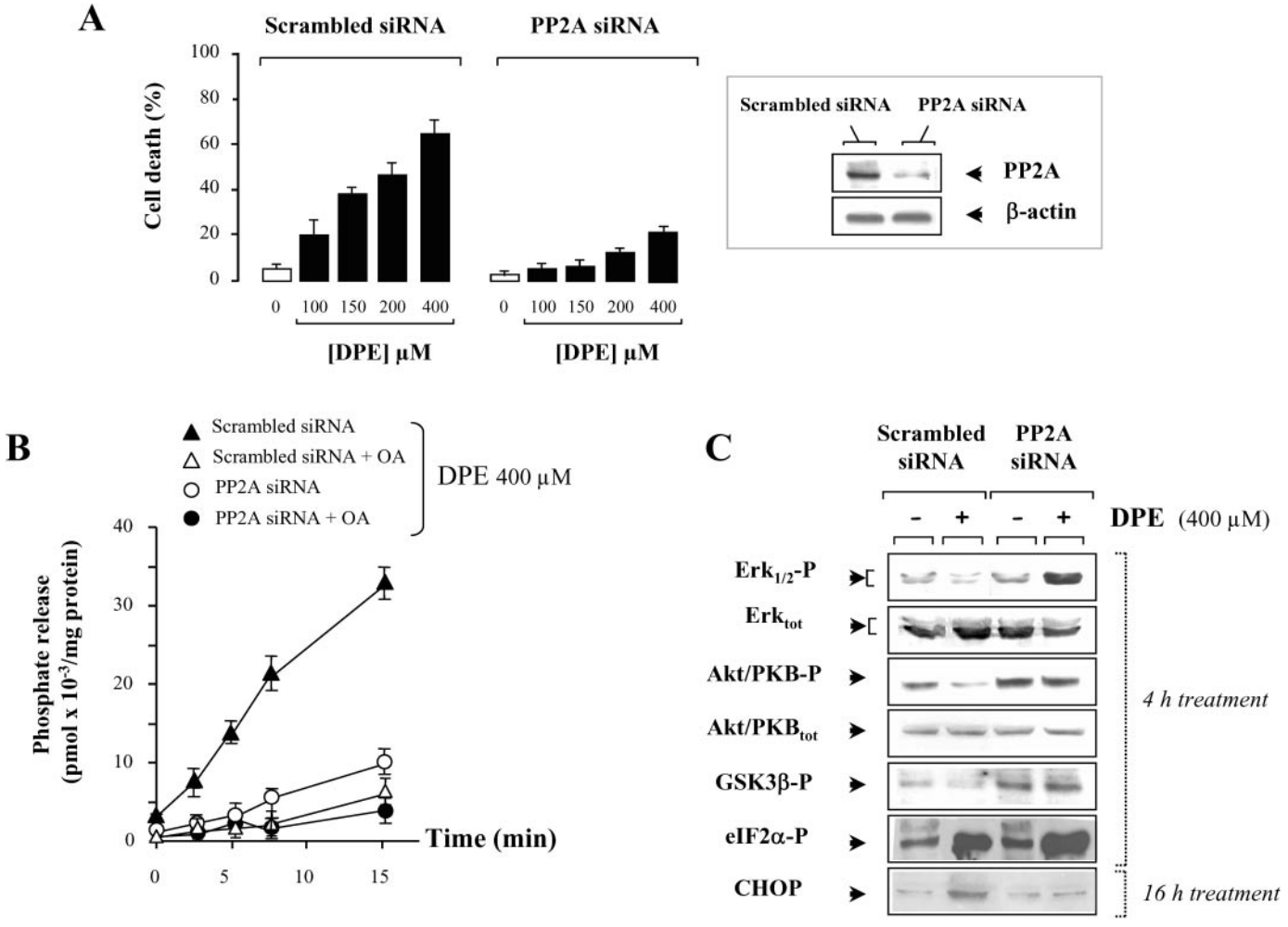

Fig. 7. Silencing of PP2A expression by RNA interference protects HT-29 cells from the DPE-induced apoptosis. HT-29 cells were transfected with scrambled or PP2A-C siRNA duplexes. (**A**) Scrambled and PP2A-C siRNA-transfected cells were incubated with (black bars) or without (open bars) a range of concentrations of DPE for 24 h. The percentage of cell death was measured using the Guava Nexin kit. The bars represent the mean value ± SD of triplicate measurements from three separate experiments. The levels of PP2A-C expression were determined in scrambled and PP2A-C siRNA-transfected cells by western blotting (right inset). The relative protein content of samples was determined using an anti-β-actin antibody. The western blots shown are representative of three separate experiments. (**B**) Scrambled and PP2A-C siRNA-transfected HT-29 cells were treated with 400 µM DPE for 1 h, and Ser/Thr phosphatase activity was quantified in cell homogenates using a synthetic phosphopeptide substrate in the presence or absence of 1 µM okadaic acid (OA) for various times. Results correspond to the phosphate release values ± SD of triplicate measurements from three separate experiments. (**C**) Western blot analyses using anti-$Erk_{1/2}$ phospho-specific Thr^{202} and Tyr^{204} ($Erk_{1/2}$-P), anti-$Erk_{1/2}$ (Erk_{tot}), anti-Akt/PKB phospho-specific Ser^{473} (Akt/PKB-P), anti-Akt/PKB (Akt/PKB_{tot}), anti-GSK3β phospho-specific Ser^{136} (GSK3β-P), anti-eIF2α phospho-specific Ser^{51} (eIF2α-P) and anti-CHOP/GADD153 (CHOP) antibodies were performed on scrambled and PP2A-C siRNA-transfected HT-29 cells that had been treated (+) or not (−) with 400 µM DPE for 4 or 16 h, as indicated. The western blots shown are representative of three separate experiments.

siRNA-transfected cells (Figure 7A; inset). To find out whether PP2A silencing also reduces the PP2A activity in HT-29 cells, phosphatase activity was assayed in both scrambled and PP2A-C siRNA-transfected cells treated with 400 µM DPE for 1 h. The stimulation of phosphatase activity by DPE, which was in the same range in scrambled siRNA-transfected and untransfected cell extracts (see Figure 6B), was inhibited in the presence of 1 µM okadaic acid (Figure 7B). In contrast, PP2A silencing reduced the DPE-induced phosphatase activity in PP2A-C siRNA-transfected cell homogenates by 70% (Figure 7B). This result was consistent with the loss of PP2A-C expression detected by western blotting. To further investigate the consequences of PP2A silencing on the modulation of survival transduction pathways by DPE including $Erk_{1/2}$ and Akt/PKB, the phosphorylation status of both kinases was examined in scrambled and PP2A siRNA-transfected cells treated with 400 µM DPE for 4 h. As in untransfected HT-29 cells (see Figure 5D), DPE induced the dephosphorylation of $Erk_{1/2}$ and Akt/PKB in scrambled siRNA-transfected cells (Figure 7C). In sharp contrast, DPE failed to induce the dephosphorylation process in PP2A siRNA-transfected cells, but further stimulated the phosphorylation of $Erk_{1/2}$. Moreover, the phosphorylation status of both kinases in PP2A siRNA-transfected cells was maintained at high levels after incubating with DPE for 24 h (data not shown). As also shown in Figure 7C, the stimulated Akt/PKB activity induced by PP2A silencing was correlated with higher levels of phosphorylation of a downstream target of Akt/PKB, GSK3β. These findings demonstrate that PP2A silencing blocked the dephosphorylation of $Erk_{1/2}$ and Akt/PKB induced by DPE, which in turn promoted cell survival. We next investigated whether silencing of PP2A affects the ER stress-dependent adaptive and apoptotic responses triggered by DPE. To do this, the phosphorylation status of eIF2α and the expression

of CHOP were checked by western blotting in scrambled and PP2A siRNA-transfected cells treated with 400 μM DPE for 4 h or 16 h, respectively. As shown in Figure 7C, PP2A silencing did not prevent the DPE-induced phosphorylation of eIF2α. Moreover, DPE induced a slight increase in the phosphorylation of eIF2α in PP2A siRNA-transfected cells as compared with scrambled siRNA-transfected cells. In sharp contrast, silencing of PP2A prevented the DPE-dependent expression of CHOP observed in scrambled siRNA-transfected or untransfected cells (see Figure 4D). These data indicate that DPE could trigger an ER stress-dependent adaptive response independently of its effect on PP2A activity, and that DPE-mediated PP2A activation is a critical checkpoint in the cell death response.

Discussion

The fate of cells subjected to ER stress depends on the balance between cell adaptive and cell death responses. ER stress has an overall protective role in tumor development by activating elements of the adaptive stress response and by attenuating apoptotic pathways. However, forced activation of ER stress can lead to the reactivation of ER stress-dependent apoptotic pathways to retard tumor development, growth and invasion (9). In the present study, we show that DPE, a major anti-oxidant compound of olive oil, alters cell proliferation and survival of colon cancer HT-29 cells by modulating the ER stress-dependent signaling pathways. DPE induces mitochondria-mediated apoptosis, which is characterized by the fall in mitochondrial membrane potential, the release of cytochrome *c* and caspase 3 activation in HT-29 cells at concentrations showed to be non-toxic in non-tumoral intestinal cells (data not shown), and markedly lower than those used by other investigators (26,28). The underlying mechanisms by which polyphenols modify the integrity of mitochondria still remain speculative. We provide evidence that DPE stimulates the expression of the pro-apoptotic proteins Bad, Bak and Bax, and represses the expression of anti-apoptotic Bcl-2. Some of these effects on the modulation of pro- and anti-apoptotic proteins by DPE have been reported for other polyphenols, such as resveratrol (44,45) and epigallocatechin (13,46). Scorrano *et al*. (47) showed that the apoptotic gateway proteins Bax and Bak are required to maintain Ca^{2+} homeostasis in the ER. Overexpression of these proteins leads to release of ER Ca^{2+} pools, and of cytochrome *c* from mitochondria and to the induction of calpain (48), and ER stress-dependent caspase 12 (8) activities. DPE also induces rapid thapsigargin-sensitive release of ER Ca^{2+} pools in HT-29 cells which, under certain circumstances, is known to promote the induction of UPR (49).

Here, we show that the DPE-induced apoptosis is the consequence of a disruption of ER homeostasis, and of the activation of UPR signaling pathways. DPE induces time-dependent activation of the ER stress sensor protein kinase, Ire1, which resulted in XBP-1 splicing and subsequent overexpression of the ER chaperone GRP78/Bip (Figure 8). Furthermore, DPE induces the phosphorylation of the ER transducer protein kinase, PERK, which in turn activates eIF2α, which is required for the attenuation of protein synthesis. Activation of apoptosis by DPE was further confirmed by the fact that the expression of the pro-apoptotic factor CHOP/GADD153 and of the Ire1-dependent JNK, both of which are implicated in promoting apoptotic effects (7), are increased and in the jun/fos AP-1 complex activation (6,50)

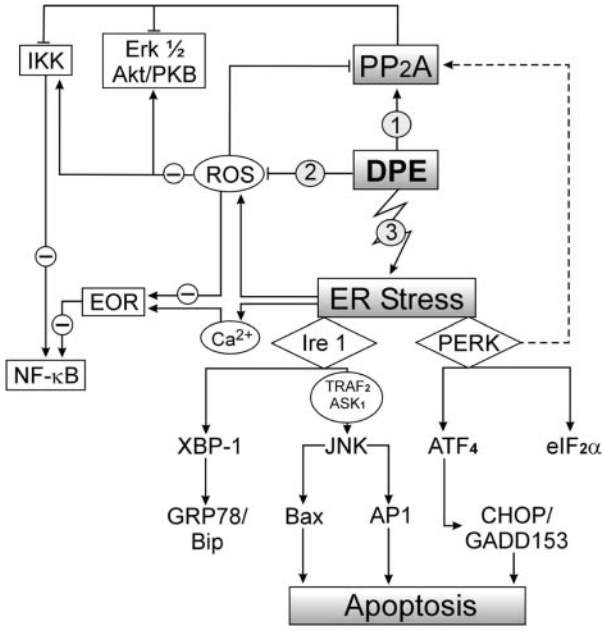

Fig. 8. Scheme of the transduction pathways involved in DPE-induced apoptosis of HT-29 cells. Schematic model representing the various signaling pathways modulated by DPE. Three non-exclusive hypotheses can account for the effect of DPE on apoptosis in colon cancer cells. (1) DPE specifically activates PP2A (2) DPE indirectly activates PP2A activity by scavenging ROS, which are known to inhibit PP2A activity, (3) DPE-induced ER stress is responsible for the increase in PP2A activity by enhancing the PERK signaling pathway (dotted line). (−) corresponds to DPE-dependent inhibition of selected pathways.

(Figure 8). We also show that DPE induces the AP-1 transcriptional activity in a similar way to that obtained in TNF-α treated cells associated with overexpression of the NAD(P)H oxidase homolog Nox-4. We have recently shown that 7-ketocholesterol, an oxysterol involved in the pathogenesis of atherosclerosis, promotes Nox-4 expression by stimulating the Ire1/JNK/AP-1 signaling pathway in smooth muscle cells (34). Silencing of Ire1 by a siRNA strategy or by inhibiting JNK activity both suppresses Nox-4 expression and protects cells against oxysterol-induced cell death. It suggests that DPE triggers AP-1-dependent expression of Nox-4, which in turn contributes to the activation of pro-apoptotic signaling pathways. Further experiments will be necessary to establish the functional relevance of the Ire1/JNK/AP-1/Nox-4 signaling pathway activation in regulating DPE-induced apoptosis.

One question addressed in this study is that of how DPE disrupts ER homeostasis and initiates the apoptotic responses in colon cancer cells. One attractive hypothesis is that DPE could alter the redox potential of the ER by its antioxidant capacity, thereby preventing oxidative protein folding and causing malfolded protein accumulation in the ER and subsequent UPR. Another non-mutually exclusive possibility is that DPE modulates different signaling pathways, such as NF-κB, Akt/PKB and $Erk_{1/2}$, that are sensitive to oxidation. The activation of NF-κB and its associated IKK is in most cases dependent on the production of ROS (51,52), and represents an important factor contributing to the deregulated growth and the resistance to apoptosis exhibited by many cancer cell types (53). Here, we show that DPE prevents TNF-α-dependent NF-κB activation by triggering the dephosphorylation of the IKK complex (Figure 8).

The downregulation of IKK and subsequent NF-κB inhibition may be dependent on the ROS scavenging capacity of DPE (Figure 8). Other antioxidants have been reported to block NF-κB activation, and the involvement of ROS is postulated to regulate the activity of the upstream kinases that converge towards the NF-κB signaling pathway. For example, pyrrolidinethiocarbamate (PDTC), *N*-acetylcysteine (NAc) and epigallocatechin have all been shown to inhibit the IKK phosphorylation in endothelial (54) and intestinal epithelial IEC-6 cells (55), respectively. Other ROS-sensitive signaling pathways including PI3K/Akt/PKB and MEK/$Erk_{1/2}$ have been shown to be involved in the regulation of NF-κB activation (for review see refs 53 and 56) and play important roles in apoptotic or cell survival processes (for review see ref. 57). The present findings demonstrate that DPE rapidly inhibits Akt/PKB activity, and induces an early and transient $Erk_{1/2}$ activation (Figure 8). Although $Erk_{1/2}$ activation may have a pro-apoptotic influence, in most cases it provides cell survival signals. Thus, it is probable that the kinetics and duration of $Erk_{1/2}$ activation determine whether it has a pro-apoptotic or anti-apoptotic effect. The role of Akt/PKB and $Erk_{1/2}$ in the regulation of ER stress-induced apoptosis has not been yet fully characterized. Hu *et al*. (39) have recently demonstrated that both Akt/PKB and MEK/$Erk_{1/2}$ signaling pathways are activated during thapsigargin- or tunicamycin-induced ER stress, and that they govern cell survival during ER stress by directly counteracting ER stress-induced apoptosis. Recently, Nguyen *et al*. (58) have provided several lines of evidence that ER-asssociated Nck-1 represses $Erk_{1/2}$ activation via an Ire1-dependent mechanism, and that Nck-1 *null* cells elicit a stronger $Erk_{1/2}$ activation in response to ER stress that is correlated with enhanced survival phenotype.

In the present study, DPE elicited a broad range of effects that interfere with signaling pathways, which control cell proliferation and/or cell death. The most intriguing effect was related to dephosphorylation of key proteins, tilting the apoptotic-survival balance towards apoptosis. Ser/Thr phosphatases, some of which are known as tumor suppressors (for review see ref. 59), regulates many cellular processes, including different signal transduction pathways, cell cycle progression, DNA replication, Wnt signaling, tumorigenesis and protein translation (40,60,61). Loss of function of such phosphatases has been shown to confer resistance on apoptotic inducing agents by activating survival pathways. We therefore postulated that Ser/Thr phosphatases might be involved in dephosphorylation process of DPE-induced signaling pathways in colon cancer HT-29 cells. We show that the inhibition of PP2A, by treating cells with either okadaic acid or calyculin A, two well established phosphatase inhibitors, or by extinguishing the expression of PP2A-C by silencing RNA interference, resulted in significant inhibition of the cell death caused by DPE. Although we did not test the effect of siRNA directed against the scaffolding A and regulatory B subunits of PP2A, other studies have shown that downregulation of PP2A-Aα subunit by RNA interference destabilizes other PP2A subunits in PC6-3 cells, and leads to PP2A downregulation (62). RNA interference experiments in *Drosophila* (63) have also shown that by suppressing the PR65/A subunit, the C subunit becomes unstable and is lost by degradation.

The three non-mutually exclusive hypotheses summarized in Figure 8 could account for the effect of DPE on PP2A activity, and for the consequences of this activation on apoptosis in colon cancer cells. (i) As shown in *in vitro* assays using DPE-treated cell homogenates or recombinant PP2A-C subunits, DPE specifically activates PP2A without having any effect on recombinant PP1 activity. This suggests that DPE may directly modulate PP2A activity and induce a broad spectrum of impact on cell viability. (ii) DPE can indirectly activate PP2A activity by scavenging ROS. Indeed, Ser/Thr phosphatase activities are affected by the oxidation state of redox-sensitive functional groups (64), and previous studies have clearly shown that H_2O_2 inhibits Ser/Thr phosphatases including PP2A, PP1 and calcineurin by oxidizing a metal (Zn or Fe) at the active site and/or by attacking essential cystein residue(s) (65,66). (iii) The DPE-induced ER stress may be responsible for the increase in PP2A activity by enhancing PERK signaling pathway. Using a yeast two-hybrid screen, Xu and Williams (67) reported that PKR, an interferon-induced antiviral eIF2α protein kinase which shares common homology and activity with PERK, phosphorylates the regulatory subunit B56α of PP2A and increases the activity of PP2A trimeric holoenzyme. Furthermore, PP2A has been shown to regulate the dephosphorylation of several proteins involved in translation control, such as eIF2α (68), and to modulate the phosphorylation-dependent cytoprotective effect of eIF2α during ER stress.

Overall, these results strongly suggest that DPE represents a potent chemopreventive agent that acts by triggering apoptosis and by targeting specific tumor suppressors, tumor-promoter-induced protein kinases and transcription factors. However, the physiological relevance obtained at doses 100–400 μM DPE remains in question and further experiments will be performed with lower concentrations of DPE to validate the *in vivo* effect. The potent inhibitory effect of DPE on the development of intestinal polyps is currently under investigation in Apc^{Min} mice, which develop multiple spontaneous intestinal adenomas throughout the intestinal tract. Our preliminary data provide strong evidence that DPE induces a marked decrease in the development of intestinal polyps in Apc^{Min} mice (data not shown). Further experiments will be necessary to determine whether apoptotic signaling pathways triggered by DPE *in vitro* are involved in the decrease of multiplicity of polyps in Apc^{Min} mice. Further experiments were needed to elucidate the molecular mechanisms/targets associated with the anti-tumor effects of DPE.

Acknowledgements

We would like to thank Mr J.P. Laigneau (INSERM U683) for art work, Ms N. Vadrot (University Paris VII) for FACS analysis, Prof. B. Bodo (UMR, CNRS 5154) for mass spectroscopy analysis of DPE, Dr P. Rouet-Benzineb (INSERM U410) and D. Bernuau (INSERM U327) for the gift of the NFκB-luciferase and AP-1-luciferase plasmids, respectively. This work was supported by the Institut National de la Santé et de la Recherche Médicale (INSERM), and in parts by grants from the Conseil Régional de Bourgogne (Gérard Lizard), the Association pour la Recherche sur le Cancer ARC (Cécile Guichard, postdoctoral fellowship), the Ligue Nationale contre le Cancer (Eric Ogier-Denis no. R05/75-103) and the Association François Aupetit AFA (Eric Ogier-Denis).

Conflict of Interest Statement: None declared.

References

1. Kaufman,R.J. (1999) Stress signaling from the lumen of the endoplasmic reticulum: coordination of gene transcriptional and translational controls. *Genes Dev.*, **13**, 1211–1233.

2. Kozutsumi,Y., Segal,M., Normington,K., Gething,M.J. and Sambrook,J. (1988) The presence of malfolded proteins in the endoplasmic reticulum signals the induction of glucose-regulated proteins. *Nature*, **332**, 462–464.
3. Yoshida,H., Matsui,T., Hosokawa,N., Kaufman,R.J., Nagata,K. and Mori,K. (2003) A time-dependent phase shift in the mammalian unfolded protein response. *Dev. Cell*, **4**, 265–271.
4. Kopito,R.R. (1997) ER quality control: the cytoplasmic connection. *Cell*, **88**, 427–430.
5. Pahl,H.L. and Baeuerle,P.A. (1997) The ER-overload response: activation of NF-kappa B. *Trends Biochem. Sci.*, **22**, 63–67.
6. Urano,F., Wang,X., Bertolotti,A., Zhang,Y., Chung,P., Harding,H.P. and Ron,D. (2000) Coupling of stress in the ER to activation of JNK protein kinases by transmembrane protein kinase IRE1. *Science*, **287**, 664–666.
7. Oyadomari,S. and Mori,M. (2004) Roles of CHOP/GADD153 in endoplasmic reticulum stress. *Cell Death Differ.*, **11**, 381–389.
8. Nakagawa,T., Zhu,H., Morishima,N., Li,E., Xu,J., Yankner,B.A. and Yuan,J. (2000) Caspase-12 mediates endoplasmic-reticulum-specific apoptosis and cytotoxicity by amyloid-beta. *Nature*, **403**, 98–103.
9. Ma,Y. and Hendershot,L.M. (2004) The role of the unfolded protein response in tumour development: friend or foe? *Nat. Rev. Cancer*, **4**, 966–977.
10. Aggarwal,B.B., Bhardwaj,A., Aggarwal,R.S., Seeram,N.P., Shishodia,S. and Takada,Y. (2004) Role of resveratrol in prevention and therapy of cancer: preclinical and clinical studies. *Anticancer Res.*, **24**, 2783–2840.
11. Kris-Etherton,P.M., Hecker,K.D., Bonanome,A., Coval,S.M., Binkoski,A.E., Hilpert,K.F., Griel,A.E. and Etherton,T.D. (2002) Bioactive compounds in foods: their role in the prevention of cardiovascular disease and cancer. *Am. J. Med.*, **113** (Suppl. 9B), 71S–88S.
12. Bode,A.M. and Dong,Z. (2004) Cancer prevention by food factors through targeting signal transduction pathways. *Nutrition*, **20**, 89–94.
13. Sah,J.F., Balasubramanian,S., Eckert,R.L. and Rorke,E.A. (2004) Epigallocatechin-3-gallate inhibits epidermal growth factor receptor signaling pathway. Evidence for direct inhibition of ERK1/2 and AKT kinases. *J. Biol. Chem.*, **279**, 12755–12762.
14. Vayalil,P.K. and Katiyar,S.K. (2004) Treatment of epigallocatechin-3-gallate inhibits matrix metalloproteinases-2 and -9 via inhibition of activation of mitogen-activated protein kinases, c-jun and NF-kappaB in human prostate carcinoma DU-145 cells. *Prostate*, **59**, 33–42.
15. Lamy,S., Gingras,D. and Beliveau,R. (2002) Green tea catechins inhibit vascular endothelial growth factor receptor phosphorylation. *Cancer Res.*, **62**, 381–385.
16. Mackenzie,G.G., Carrasquedo,F., Delfino,J.M., Keen,C.L., Fraga,C.G. and Oteiza,P.I. (2004) Epicatechin, catechin, and dimeric procyanidins inhibit PMA-induced NF-kappaB activation at multiple steps in Jurkat T cells. *FASEB J.*, **18**, 167–169.
17. Ermakova,S., Choi,B.Y., Choi,H.S., Kang,B.S., Bode,A.M. and Dong,Z. (2005) The intermediate filament protein vimentin is a new target for epigallocatechin gallate. *J. Biol. Chem.*, **280**, 16882–16890.
18. Jang,M., Cai,L., Udeani,G.O. *et al.* (1997) Cancer chemopreventive activity of resveratrol, a natural product derived from grapes. *Science*, **275**, 218–220.
19. Kuper,H., Tzonou,A., Lagiou,P., Mucci,L.A., Trichopoulos,D., Stuver,S.O. and Trichopoulou,A. (2000) Diet and hepatocellular carcinoma: a case–control study in Greece. *Nutr. Cancer*, **38**, 6–12.
20. Trichopoulou,A., Katsouyanni,K., Stuver,S., Tzala,L., Gnardellis,C., Rimm,E. and Trichopoulos,D. (1995) Consumption of olive oil and specific food groups in relation to breast cancer risk in Greece. *J. Natl Cancer Inst.*, **87**, 110–116.
21. Martin-Moreno,J.M., Willett,W.C., Gorgojo,L., Banegas,J.R., Rodriguez-Artalejo,F., Fernandez-Rodriguez,J.C., Maisonneuve,P. and Boyle,P. (1994) Dietary fat, olive oil intake and breast cancer risk. *Int. J. Cancer*, **58**, 774–780.
22. Grignaffini,P., Roma,P., Galli,C. and Catapano,A.L. (1994) Protection of low-density lipoprotein from oxidation by 3,4-dihydroxyphenylethanol. *Lancet*, **343**, 1296–1297.
23. Petroni,A., Blasevich,M., Salami,M., Servili,M., Montedoro,G.F. and Galli,C. (1994) A phenolic antioxidant extracted from olive oil inhibits platelet aggregation and arachidonic acid metabolism *in vitro*. *World Rev. Nutr. Diet*, **75**, 169–172.
24. O'Dowd,Y., Driss,F., Dang,P.M., Elbim,C., Gougerot-Pocidalo,M.A., Pasquier,C. and El-Benna,J. (2004) Antioxidant effect of hydroxytyrosol, a polyphenol from olive oil: scavenging of hydrogen peroxide but not superoxide anion produced by human neutrophils. *Biochem. Pharmacol.*, **68**, 2003–2008.
25. Manna,C., Galletti,P., Maisto,G., Cucciolla,V., D'Angelo,S. and Zappia,V. (2000) Transport mechanism and metabolism of olive oil hydroxytyrosol in Caco-2 cells. *FEBS Lett*, **470**, 341–344.
26. Ragione,F.D., Cucciolla,V., Borriello,A., Pietra,V.D., Pontoni,G., Racioppi,L., Manna,C., Galletti,P. and Zappia,V. (2000) Hydroxytyrosol, a natural molecule occurring in olive oil, induces cytochrome c-dependent apoptosis. *Biochem. Biophys. Res. Commun.*, **278**, 733–739.
27. Della Ragione,F., Cucciolla,V., Criniti,V., Indaco,S., Borriello,A. and Zappia,V. (2002) Antioxidants induce different phenotypes by a distinct modulation of signal transduction. *FEBS Lett.*, **532**, 289–294.
28. Fabiani,R., De Bartolomeo,A., Rosignoli,P., Servili,M., Montedoro,G.F. and Morozzi,G. (2002) Cancer chemoprevention by hydroxytyrosol isolated from virgin olive oil through G_1 cell cycle arrest and apoptosis. *Eur. J. Cancer Prev.*, **11**, 351–358.
29. de la Puerta,R., Ruiz Gutierrez,V. and Hoult,J.R. (1999) Inhibition of leukocyte 5-lipoxygenase by phenolics from virgin olive oil. *Biochem. Pharmacol.*, **57**, 445–449.
30. de la Puerta,R., Martinez Dominguez,M.E., Ruiz-Gutierrez,V., Flavill,J.A. and Hoult,J.R. (2001) Effects of virgin olive oil phenolics on scavenging of reactive nitrogen species and upon nitrergic neurotransmission. *Life Sci.*, **69**, 1213–1222.
31. Bolender,R.P., Paumgartner,D., Muellener,D., Losa,G. and Weibel,E.R. (1980) Integrated stereological and biochemical studies on hepatocytic membranes. I.V. Heterogeneous distribution of marker enzymes on endoplasmic reticulum membranes in fractions. *J. Cell Biol.*, **85**, 577–586.
32. Ma,Y. and Hendershot,L.M. (2004) Herp is dually regulated by both the endoplasmic reticulum stress-specific branch of the unfolded protein response and a branch that is shared with other cellular stress pathways. *J. Biol. Chem.*, **279**, 13792–13799.
33. McCullough,K.D., Martindale,J.L., Klotz,L.O., Aw,T.Y. and Holbrook,N.J. (2001) Gadd153 sensitizes cells to endoplasmic reticulum stress by down-regulating Bcl2 and perturbing the cellular redox state. *Mol. Cell. Biol.*, **21**, 1249–1259.
34. Pedruzzi,E., Guichard,C., Ollivier,V. *et al.* (2004) NAD(P)H oxidase Nox-4 mediates 7-ketocholesterol-induced endoplasmic reticulum stress and apoptosis in human aortic smooth muscle cells. *Mol. Cell. Biol.*, **24**, 10703–10717.
35. Tsuruta,F., Sunayama,J., Mori,Y., Hattori,S., Shimizu,S., Tsujimoto,Y., Yoshioka,K., Masuyama,N. and Gotoh,Y. (2004) JNK promotes Bax translocation to mitochondria through phosphorylation of 14-3-3 proteins. *EMBO J.*, **23**, 1889–1899.
36. Tobiume,K., Matsuzawa,A., Takahashi,T., Nishitoh,H., Morita,K., Takeda,K., Minowa,O., Miyazono,K., Noda,T. and Ichijo,H. (2001) ASK1 is required for sustained activations of JNK/p38 MAP kinases and apoptosis. *EMBO Rep.*, **2**, 222–228.
37. Baldwin,A.S. Jr (1996) The NF-kappa B and I kappa B proteins: new discoveries and insights. *Annu. Rev. Immunol.*, **14**, 649–683.
38. Karin,M. and Ben-Neriah,Y. (2000) Phosphorylation meets ubiquitination: the control of NF-[kappa]B activity. *Annu. Rev. Immunol.*, **18**, 621–663.
39. Hu,P., Han,Z., Couvillon,A.D. and Exton,J.H. (2004) Critical role of endogenous Akt/IAPs and MEK1/ERK pathways in counteracting endoplasmic reticulum stress-induced cell death. *J. Biol. Chem.*, **279**, 49420–49429.
40. Janssens,V. and Goris,J. (2001) Protein phosphatase 2A: a highly regulated family of serine/threonine phosphatases implicated in cell growth and signalling. *Biochem. J.*, **353**, 417–439.
41. Moreno,C.S., Park,S., Nelson,K., Ashby,D., Hubalek,F., Lane,W.S. and Pallas,D.C. (2000) WD40 repeat proteins striatin and S/G(2) nuclear autoantigen are members of a novel family of calmodulin-binding proteins that associate with protein phosphatase 2A. *J. Biol. Chem.*, **275**, 5257–5263.
42. Fellner,T., Lackner,D.H., Hombauer,H., Piribauer,P., Mudrak,I., Zaragoza,K., Juno,C. and Ogris,E. (2003) A novel and essential mechanism determining specificity and activity of protein phosphatase 2A (PP2A) *in vivo*. *Genes Dev.*, **17**, 2138–2150.
43. Ogris,E., Du,X., Nelson,K.C., Mak,E.K., Yu,X.X., Lane,W.S. and Pallas,D.C. (1999) A protein phosphatase methylesterase (PME-1) is one of several novel proteins stably associating with two inactive mutants of protein phosphatase 2A. *J. Biol. Chem.*, **274**, 14382–14391.
44. Mahyar-Roemer,M., Kohler,H. and Roemer,K. (2002) Role of Bax in resveratrol-induced apoptosis of colorectal carcinoma cells. *BMC Cancer*, **2**, 27.
45. Delmas,D., Rebe,C., Lacour,S. *et al.* (2003) Resveratrol-induced apoptosis is associated with Fas redistribution in the rafts and the formation of a death-inducing signaling complex in colon cancer cells. *J. Biol. Chem.*, **278**, 41482–41490.
46. Hastak,K., Gupta,S., Ahmad,N., Agarwal,M.K., Agarwal,M.L. and Mukhtar,H. (2003) Role of p53 and NF-kappaB in epigallocatechin-3-gallate-induced apoptosis of LNCaP cells. *Oncogene*, **22**, 4851–4859.

47. Scorrano,L., Oakes,S.A., Opferman,J.T., Cheng,E.H., Sorcinelli,M.D., Pozzan,T. and Korsmeyer,S.J. (2003) BAX and BAK regulation of endoplasmic reticulum Ca2+: a control point for apoptosis. *Science*, **300**, 135–139.
48. Wang,K.K. (2000) Calpain and caspase: can you tell the difference? *Trends Neurosci.*, **23**, 20–26.
49. Treiman,M. (2002) Regulation of the endoplasmic reticulum calcium storage during the unfolded protein response—significance in tissue ischemia? *Trends Cardiovasc. Med.*, **12**, 57–62.
50. Ubeda,M., Vallejo,M. and Habener,J.F. (1999) CHOP enhancement of gene transcription by interactions with Jun/Fos AP-1 complex proteins. *Mol. Cell. Biol.*, **19**, 7589–7599.
51. Manna,S.K., Zhang,H.J., Yan,T., Oberley,L.W. and Aggarwal,B.B. (1998) Overexpression of manganese superoxide dismutase suppresses tumor necrosis factor-induced apoptosis and activation of nuclear transcription factor-kappaB and activated protein-1. *J. Biol. Chem.*, **273**, 13245–13254.
52. Manna,S.K., Kuo,M.T. and Aggarwal,B.B. (1999) Overexpression of gamma-glutamylcysteine synthetase suppresses tumor necrosis factor-induced apoptosis and activation of nuclear transcription factor-kappa B and activator protein-1. *Oncogene*, **18**, 4371–4382.
53. Nakanishi,C. and Toi,M. (2005) Nuclear factor-kappaB inhibitors as sensitizers to anticancer drugs. *Nat. Rev. Cancer*, **5**, 297–309.
54. Spiecker,M., Darius,H., Kaboth,K., Hubner,F. and Liao,J.K. (1998) Differential regulation of endothelial cell adhesion molecule expression by nitric oxide donors and antioxidants. *J. Leukoc. Biol.*, **63**, 732–739.
55. Yang,F., Oz,H.S., Barve,S., de Villiers,W.J., McClain,C.J. and Varilek,G.W. (2001) The green tea polyphenol (−)-epigallocatechin-3-gallate blocks nuclear factor-kappa B activation by inhibiting I kappa B kinase activity in the intestinal epithelial cell line IEC-6. *Mol. Pharmacol.*, **60**, 528–533.
56. Kundu,J.K. and Surh,Y.J. (2004) Molecular basis of chemoprevention by resveratrol: NF-kappaB and AP-1 as potential targets. *Mutat. Res.*, **555**, 65–80.
57. Lee,J.T.Jr and McCubrey,J.A. (2002) The Raf/MEK/ERK signal transduction cascade as a target for chemotherapeutic intervention in leukemia. *Leukemia*, **16**, 486–507.
58. Nguyen,D.T., Kebache,S., Fazel,A. *et al.* (2004) Nck-dependent activation of extracellular signal-regulated kinase-1 and regulation of cell survival during endoplasmic reticulum stress. *Mol. Biol. Cell*, **15**, 4248–4260.
59. Janssens,V., Goris,J. and Van Hoof,C. (2005) PP2A: the expected tumor suppressor. *Curr. Opin. Genet Dev.*, **15**, 34–41.
60. Virshup,D.M. (2000) Protein phosphatase 2A: a panoply of enzymes. *Curr. Opin. Cell Biol.*, **12**, 180–185.
61. Schonthal,A.H. (2001) Role of serine/threonine protein phosphatase 2A in cancer. *Cancer Lett.*, **170**, 1–13.
62. Strack,S., Cribbs,J.T. and Gomez,L. (2004) Critical role for protein phosphatase 2A heterotrimers in mammalian cell survival. *J. Biol. Chem.*, **279**, 47732–47739.
63. Ruediger,R., Pham,H.T. and Walter,G. (2001) Disruption of protein phosphatase 2A subunit interaction in human cancers with mutations in the A alpha subunit gene. *Oncogene*, **20**, 10–15.
64. Rusnak,F. and Reiter,T. (2000) Sensing electrons: protein phosphatase redox regulation. *Trends Biochem. Sci.*, **25**, 527–529.
65. Sommer,D., Coleman,S., Swanson,S.A. and Stemmer,P.M. (2002) Differential susceptibilities of serine/threonine phosphatases to oxidative and nitrosative stress. *Arch. Biochem. Biophys.*, **404**, 271–278.
66. Rao,R.K. and Clayton,L.W. (2002) Regulation of protein phosphatase 2A by hydrogen peroxide and glutathionylation. *Biochem. Biophys. Res. Commun.*, **293**, 610–616.
67. Xu,Z. and Williams,B.R. (2000) The B56alpha regulatory subunit of protein phosphatase 2A is a target for regulation by double-stranded RNA-dependent protein kinase PKR. *Mol. Cell. Biol.*, **20**, 5285–5299.
68. Chen,S.C., Kramer,G. and Hardesty,B. (1989) Isolation and partial characterization of an Mr 60,000 subunit of a type 2A phosphatase from rabbit reticulocytes. *J. Biol. Chem.*, **264**, 7267–7275.

Received December 16, 2005; revised February 13, 2006; accepted March 3, 2006